Studying surfactant mass transport through dynamic interfacial tension measurements: A review of the models, experiments, and the contribution of microfluidics

Camille Brigodiot, Marie Marsiglia, Christine Dalmazzone, Karin Schroën, Annie Colin

Advances in Colloid and Interface Science 331 (2024) 103239

Contents lists available at ScienceDirect

Advances in Colloid and Interface Science

journal homepage: www.elsevier.com/locate/cis

Historical Perspective

Studying surfactant mass transport through dynamic interfacial tension measurements: A review of the models, experiments, and the contribution of microfluidics

Camille Brigodiot [a], Marie Marsiglia [a,*], Christine Dalmazzone [a], Karin Schroën [b], Annie Colin [c]

[a] IFP Energies nouvelles (IFPEN), 1-4 avenue de Bois-Préau, 92852 Rueil-Malmaison Cedex, France
[b] Wageningen University and Research (WUR), Wageningen, the Netherlands
[c] ESPCI Paris, Paris, France

ARTICLE INFO

Keywords:
Interfacial tension
Surfactant mass transport
Microfluidics
Adsorption kinetics
Diffusion

ABSTRACT

Surfactant mass transport towards an interface plays a critical role during formation of emulsions, foams and in industrial processes where two immiscible phases coexist. The understanding of these mechanisms as experimentally observed by dynamic interfacial tension measurements, is crucial. In this review, theoretical models describing both equilibrated systems and surfactant kinetics are covered. Experimental results from the literature are analysed based on the nature of surfactants and the tensiometry methods used. The innovative microfluidic techniques that have become available to study both diffusion and adsorption mechanisms during surfactant mass transport are discussed and compared with classical methods. This review focuses on surfactant transport during formation of droplets or bubbles; stabilisation of dispersed systems is not discussed here.

1. Introduction

Have you ever observed any of these phenomena in your daily life? Insects that walk on water, dew that beads on flower petals, sugar that soaks coffee or a drop of water that hangs without falling? These amusing facts are all the result of the surface tension of liquids [1,2]. This physico-chemical phenomenon is linked to the molecular interactions of a fluid, i.e. the way its molecules are attracted to each other, as well as how they interact with molecules from another material or liquid. The molecules of a fluid exert forces of attraction (Van der Waals) or repulsion (electrostatic, steric) on each other. In a system involving several media, molecular interactions are unbalanced: molecules at the interface interact with those in the other medium, but those in the material interact only with their own. The system naturally tends towards an equilibrium corresponding to the least energetic configuration. It then modifies its geometry to reduce the surface area of the interface with the other medium. The force that maintains the system in this configuration is due to surface interfacial tension (IFT) or, when the interface is formed with air, it is often called"surface tension" (SFT). Interfacial tension, noted (γ) is the energy per unit area required to create an interface, measured in (J/m^2). γ is also defined by the Gibbs free energy (dG) expressed as $dG = \gamma dA$, where dA represents the change in surface area measured in square meters m^2. The study of surface phenomena dates back several centuries, with Laplace (1749–1827) and Young (1773–1829) being key contributors. Bouasse's book in 1924 [3] provides insights into their work.

Surface tension governs the behaviour of interfaces between immiscible phases, a key factor in many natural and industrial phenomena. The ability of life to thrive on the Earth's continents is intimately linked to water's surface tension, which is around 72 $mN.m^{-1}$ [4]. This fundamental physical property has a major influence on the Earth's water cycle and on the origin of precipitation essential to life. For instance, if this value were twice as low, persistent fog would obscure large parts of the globe, hindering sunlight and altering the Earth's albedo, raindrops would be larger, bubbles would form on coastlines. The delicate balance of life on Earth is partly due to this precise value of surface tension [5]. When it comes to industrial processes, understanding the behaviour of interfaces between immiscible phases is of paramount importance. Without giving an exhaustive list, surface tension influences the adhesion of paints and varnishes to surfaces [6]. Appropriate surface tensions are necessary to ensure uniform coverage. In the printing industry, the surface tension of inks and substrates is crucial to achieving quality prints [7,8]. Active spraying and aerosols are commonly used in agriculture (for pesticides and herbicides) [9], the

* Corresponding author.
E-mail address: marie.marsiglia@ifpen.fr (M. Marsiglia).

https://doi.org/10.1016/j.cis.2024.103239
Received in revised form 14 June 2024;
Available online 20 June 2024

automotive industry (for paints and coatings) and household products (such as cleaning agents and insecticides). Surface tension governs the wetting and spreading properties of spray droplets.

In other various industries including food, pharmaceuticals, cosmetics, or for environmental purification, many processes rely on interface formation and stability, governed by interfacial tension. For instance, liquid-liquid extraction is a separation process widely used in these industries involving the transfer of a solute (or several solutes) from one liquid phase to another immiscible liquid phase. It necessitates precise control over interface formation and stability, which are primarily dictated by interfacial tension. Finally, surface tension is at the origin of the Rayleigh-Plateau mechanism for droplet and bubble formation. It plays a fundamental role in emulsification and spraying processes used in these industries.

For all these processes, it is important to control and especially tailor interfacial tension. This is possible by using surfactant molecules. A surfactant, also referred to as a surface-active agent, consists of two functional components: a nonpolar hydrophobic tail that is soluble in oil and a polar hydrophilic head that is soluble in water. Typically, the hydrophobic segment comprises a lengthy hydrocarbon chain (either linear or branched), a fluorocarbon, a siloxane chain, or a short polymer chain. The hydrophilic portion can be created through moieties, with the surfactants being categorised based on the ionic nature of these fractions into four types: anionic, cationic, nonionic, and amphoteric (or zwitterionic). Amphiphilic molecules modify the molecular interactions between two liquids by adsorbing at interfaces, reducing the repulsive forces between fluids or solids, and stabilising the system by reducing its energy. This reduction in energy manifests itself as a decrease in the interfacial or surface tension (IFT or SFT) of the system. The reduction in interfacial or surface tension is directly related to the number of molecules adsorbed (surfactant mass transfer) at the interfaces, and varies over time until equilibrium is reached. Classical surfactants reduce water-air or water-oil surface tension by 30–40 $mN.m^{-1}$.

In real-world applications, many processes involve the dynamic movement of interfaces rather than their static equilibrium. This brings us to the fascinating field of dynamic interfacial tension (DIFT), a specialised area of study that looks at the evolution of forces at interfaces during dynamic processes. Dynamic interfacial tension not only broadens our understanding of intermolecular forces and surface interactions, but also provides valuable insights into the kinetics and thermodynamics of complex systems. It examines how interfacial tension evolves over time, particularly when subjected to external forces or when different phases are in relative motion. When an interface is created between two different phases, two liquids, at short time, the interface is naked and its surface tension is high. It is the one which acts between the two pure liquids or phases in absence of surfactants. It takes time for the surfactant molecules to reach the interface, orientate themselves and adsorb to it.

In the pharmaceutical, cosmetic and food [10] industries, there is a need to stabilise emulsions and foams products from the formation of the systems and through time. Therefore, surfactants are added to control the stability of these systems first at short time since droplets or bubbles are formed between 8 μs [11,12] and 30 ms [13] according to the method used, and secondly at long time to control ageing process. Schroën et al. [14] have highlighted the relevance of knowing the DIFT at short time to have a correct comprehension of the droplets or bubbles stability at the characteristic time scale and length scale of formation and first collisions. This measurement can be quite difficult since the time scale is very small and the predominant mass transfer mechanism depends on the droplet size [15]. Moreover, over longer time, emulsions and foams are proned to different ageing processes such as coalescence, Ostwald ripening, floculation, or phase inversion [14]. Therefore, surfactants must be chosen considering both their adsorption dynamics and their impact on interfacial properties in order to mitigate ageing effects. Besides emulsification processes, in wastewater treatment [16,17], emulsion-breaking agents (or demulsifiers) [18] are widely used to separate and recover contaminants coming from oil industry [19,20], or pharmaceutical industry [21,22]. These molecules have the ability to disturb the interface by reversing the droplets curvature and promote coalescence [23]. These molecules are also used in emerging processes for wastewater treatment such as pickering emulsions [24,25].

The theoretical models behind these phenomena are far from trivial and have been a subject of interest for decades. Modeling the transfer of matter from the bulk volume to the interface, the kinetics of the adsorption, and the flows are necessary to understand what the value of the surface tension is over time and to characterise the efficiency of the surfactants. This knowledge is vital for improving our ability to design and optimize the previous processes. Measuring dynamic surface tension to be able to design a process is not simply a matter of creating an interface and monitoring the evolution of surface tension over time. Indeed, to be relevant, the approach must be based on the same conditions of material input and flow. To predict the action of a surfactant in a process, for example when spraying plant protection additives, you need to put the surfactants into action under conditions similar to the process in terms of material transfer, flow and adsorption kinetics. In practice, this is very complex. So there is a two-stage answer to the problem. First, we need to define the relevant characteristic time for the process: typically 0.1 to 10 milliseconds for drop formation in a high pressure homogeniser [14], 10 milliseconds for drop formation using a direct membrane emulsification process [26], 0.1 to 100 s in a colloidal mill [13], a second for the rebound of drops on a surface, a second or several seconds in paint spreading processes or during drop formation in liquid-liquid extraction processes [27–29]. The surface tension should then be measured during the interface creation time in a device that mimics the supply of material. Note that while the dynamic interfacial phenomenon has been extensively studied in the literature for time above one second [30], the measurement of dynamic interfacial tension (DIFT) at shorter time (subsecond) remains challenging and has received limited attention. However, interfacial properties, especially dynamic interfacial tension (DIFT), play a fundamental role in various industrial processes involving interface formation, such as emulsions [31–33] and foams [34]. As mimicking the input of material is complex, it will be more straightforward and rigorous to run numerical simulations to simulate the process. This would be the second step to accurately answer the problem, and it requires a thorough knowledge of surfactant state laws, adsorption kinetics, diffusion coefficients and phase partitioning.

In this review article, we believe that this point of view is the key to solving these problems and tackling surfactant mass transport in a new way. We believe that knowledge of these interfacial data is fundamental, especially for accurately predict surfactant action in processes. We review ways of measuring them independently. In section 2, classical theoretical models for equilibrium and dynamic systems are presented and in section 3, a synthetic analysis of experiments and models describing the different phenomena is made. Finally, section 4 provides an analysis of innovative microfluidic techniques to study interfacial properties.

2. Description of surfactant mass transport and adsorption at the interface

Ward and Tordai [35] were the first to observe and study interfacial properties over time, and especially to describe the different steps introducing the sub-surface (Fig. 1). Let us start by saying that to describe the mass transport of surfactants towards an interface, one can find in the literature different vocabulary that may confuse the reader. The term"adsorption" is either used to nominate the whole mass transport of surfactant from the diffusion in the bulk to the last steps at the interface, or only to describe the final stage where the amphiphilic molecules rearrange themselves at the interface. For the sake of clarity, in this review,"adsorption" designates the last step of the whole mechanism, while"diffusion" or"convection" describes the mass transport of molecules from the bulk to the sub-interface. The kinetics of surfactants

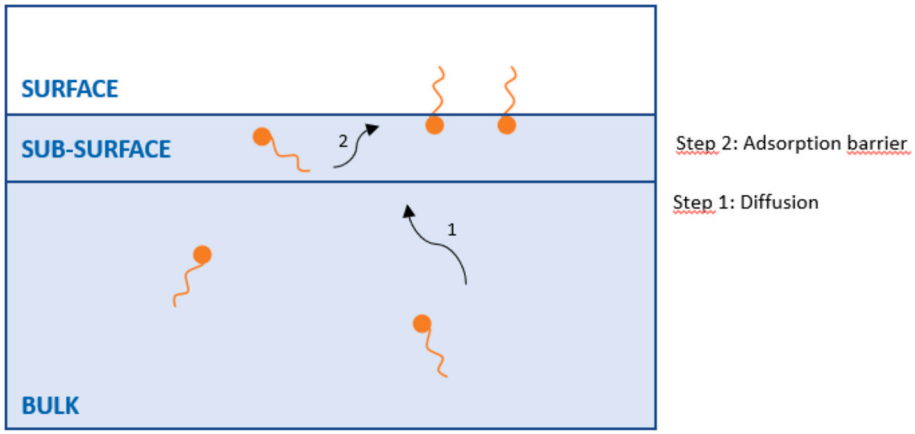

Fig. 1. Simplified scheme of surfactant mass transport mechanism towards a surface.

mass-transfer can be either limited by diffusion or convection only (first step), it is"diffusion-limited" or"diffusion-controlled". However, the adsorption step (second step) cannot always be neglected and mass-transfer kinetics of surfactant can be described as"adsorption-limited","mixed-diffusion","diffusion-kinetic","mixed-kinetic" controlled [36].

Nevertheless, these models are not always sufficient to describe properly surfactant mass transport as they usually do not consider the desorption of surfactant molecules [37,38]. When the interface concentration Γ has exceeded the equilibrium concentration Γ_0, some molecules will desorb in order to go back to an equilibrated state. This mechanism is called"back-diffusion" by Ward and Tordai [39] and can also occur in some cases before equilibrium when the interface is compressed or wrinkled.

Besides, rearrangement mechanisms can also be observed such as the formation of micelles above a critical concentration of surfactant called the critical micelle concentration (*cmc*), or even formation of micro-emulsions Winsor-type that could impact the kinetics of mass transfer [40,41]. Finally, in some cases and especially with molecules having affinities for both phases, so with a significant partition coefficient, a mass-transfer across the interface can be observed and measured [42]. These different phenomena also depend on the nature of the fluids and surfactants which is very diverse: from proteins in biology or food industry, to ionic surfactants such as SDS [43] or CTAB [44], non ionic surfactants such as Tween 80, Triton X-100 [45] and C_iE_j [46] or polymers such as PEO [47]. It is clear that the diversity in surfactant nature leads to different kinetics: a non ionic compound with a long carbon chain will not behave similarly to a smaller ionic molecule in solution. When the first system will reach equilibrium with a characteristic diffusion time caused by sterical arrangements and Van der Walls interactions, the second one will be driven by ionic forces.

In the following, we review works dealing with the theoretical description of those processes.

2.1. Adsorption isotherms at equilibrium

In this part, theoretical aspects of surfactant mass transport mechanism are presented. To describe the behaviour of surfactants at the interface, the surface excess concentration, also denominated as the concentration of surfactant at the interface, noted Γ has to be expressed with known parameters. Adsorption isotherms relate Γ to the concentration of surfactant in the bulk c. Even though the surface excess concentration is not easily measurable, it can directly be linked to the surface tension. The relation between the surface or interfacial tension γ and the concentration at the interface is called the equation of state.

It is key to study the systems at equilibrium first to extract crucial parameters such as the maximum surface excess concentration Γ_∞. In this part, we will discuss the different existing isotherms describing equilibrium.

The first model to relate Γ, the surface excess concentration expressed in mol/m^2 and the concentration in the bulk c (mol/m^3) is the linear Henry isotherm:

$$\Gamma = K_H.c \tag{1}$$

where K_H (m) is an equilibrium constant. This relation is only valid for low surface concentration and assumes that the adsorbed monomers have no interactions with each other. This relation is therefore used only for specific very simple diluted systems and cannot describe most of the surfactants in the literature.

The most used isotherm is the Langmuir [48] one. In this model, the surface is divided in equivalent adsorbing sites and it is assumed that there is no interaction between the adsorbed or adsorbing molecules. One simple way to write the Langmuir isotherm is to model adsorption as a dynamic equilibrium between adsorption and desorption from the surface. This kinetic approach gives the variation of surface concentration with time, due to adsorption as follows [49]:

$$\frac{d\Gamma}{dt} = k_a.c.\Gamma_\infty.\left(1 - \frac{\Gamma}{\Gamma_\infty}\right) - k_d.\Gamma \tag{2}$$

where k_a and k_d are the adsorption and desorption rate respectively and Γ_∞ is the maximum surface excess. k_a in $m^3/(mol.s)$ and k_d in s^{-1} are constants related to adsorption and desorption energies E_a and E_d by:

$$k_{a,d} = k^0_{a,d} exp\left(E_{a,d}/k_BT\right) \tag{3}$$

where E_a and E_d are independent of Γ. k_B is the Boltzmann constant in J/K and T the temperature of the system in K. The energies $E_{a,d}$ are in J. At equilibrium, Γ is constant so the Langmuir isotherm is written as:

$$\Gamma = \Gamma_\infty\left(\frac{K_L.c}{1 + K_L.c}\right) \tag{4}$$

The equilibrium constant $K_L = \frac{k_a}{k_d}$ is expressed as the inverse of a concentration, usually in m^3/mol. Note that this isotherm can also be derived from thermodynamic considerations as detailed by Prosser et al. [50].

Then, to obtain the relation between Γ and the surface tension γ, it is necessary to use the Gibbs fundamental equation, relating the interfacial tension variation with the chemical potentials μ_i and surface excesses Γ_i of the components in the system:

$$d\gamma_{T,P} = -\sum_i \Gamma_i d\mu_i \tag{5}$$

For a system with only one surfactant component, it is possible to

obtain the eq. (5) by expressing the chemical potential of a component as a function of chemical potential of reference and chemical activity. The Gibbs equation of the interface is written as:

$$\Gamma = -\frac{1}{RT}\left(\frac{\partial\gamma}{\partial ln(c)}\right) \tag{6}$$

where γ is the interfacial tension, R the ideal gas constant, T the temperature and where the interface is assumed ideal with no thickness.

From the Langmuir isotherm and the Gibbs equation, it is possible to obtain the Szyszkowski relation of surface state as follows:

$$\Pi = \gamma_0 - \gamma = nRT\Gamma_\infty ln(1 + K_L.c) \tag{7}$$

where Π is the surface pressure that can be experimentally measured with γ_0 the interfacial tension between the two fluids in absence of surfactant. n is a dimensionless number equal to 1 for non ionic surfactants, neutral molecules and ionic surfactants if there is an excess of electrolytes, and $n = 2$ if the latter are in stoechiometric proportion with the electrolytes, neutrality at the interface having to be maintained. From this equation of state and the measurement of interfacial tension, it is possible to deduce Γ_∞ and K_L, parameters that will be useful to study the dynamics of surfactant mass transport.

Frumkin has proposed a three-parameter model where the adsorbed monolayer is non ideal and takes into account interactions between solvent and solute molecules [50,51]. This approach is then expressed as follows:

$$c = \frac{1}{K_F}.\frac{\frac{\Gamma}{\Gamma_\infty}}{1-\frac{\Gamma}{\Gamma_\infty}}.exp\left[-A\left(\frac{\Gamma}{\Gamma_\infty}\right)\right] \tag{8}$$

or as:

$$\frac{\Gamma}{\Gamma_\infty} = \frac{c}{c + \frac{1}{K_F}exp\left(-A\frac{\Gamma}{\Gamma_\infty}\right)} \tag{9}$$

where c is the concentration of the surfactant in the bulk, K_F the Frumkin adsorption constant and A a constant that depends on the non-ideality of the interface. To obtain this equation, the same kinetic approach as before is used but in this situation, the adsorption and desorption energies depend on Γ by a power law as well demonstrated before in the literature [49,52]. The generalised Frumkin model is written as:

$$\frac{\Gamma}{\Gamma_\infty} = \frac{c}{c + \frac{1}{K_F}exp\left(-A\frac{\Gamma}{\Gamma_\infty}\right)^n} \tag{10}$$

where n is a constant and has to be determined by fitting experimental data. By applying the Gibbs relation, such as done above, the equation of state in the generalised Frumkin model can be expressed as follows:

$$\Pi = \gamma_0 - \gamma = -RT\Gamma_\infty ln\left(1-\frac{\Gamma}{\Gamma_\infty}\right) - \frac{nRTA}{n+1}\Gamma_\infty\left(\frac{\Gamma}{\Gamma_\infty}\right)^{n+1} \tag{11}$$

When $n = 1$, eq. (9) becomes simpler and is called the Frumkin model, and when $A = 0$, corresponding to an ideal interface, the Langmuir model is recovered. Contrary to the Langmuir model, numerical simulations are necessary to calculate the various parameters essential for constructing a kinetics model.

The steps of the calculations are not given here but can be found elsewhere [50,53]. The review written by Prosser et al. in 2001 [50] describes well the steps and provides analysis of the models for ionic surfactants. In 2020, the review from Wang et al. [53] also gives a detailed analysis of adsorption models, especially for adsorption at a solid surface.

Given that there is no perfect theoretical model, the concept of equilibrium is grasped by comparing various isotherms by fitting experimental equilibrium data. Then, the most suitable isotherm that accurately describes the fluid/surfactant system at equilibrium can be chosen [26,38,54–56] to determine characteristic equilibrium parameters.

The isotherms have been compared in a study in 2003 by Lin et al. [57]. They have investigated surface equation for non-ionic C_iE_j surfactants. Following previous research [58,59], the authors [57] have compared the Langmuir (L), Frumkin (F) and generalised Frumkin (GF) isotherms by plotting data of interfacial tension as a function of surfactant concentration in the bulk $\gamma(c)$ and also as a function of surface excess concentration $\gamma(\Gamma)$ (Fig. 2). F_1 curve corresponds to the Frumkin best-fit with $\gamma(ln(C))$ data and F_2 is the best-fit considering both set of equilibrium data ($\gamma(ln(C))$ and $\gamma(\Gamma)$.

According to Fig. 2, it was concluded that it is important to plot both $\gamma(ln(C))$ and $\gamma(\Gamma)$. In fact, for $C_{10}E_8$ and $C_{14}E_8$ (Fig. 2a,b), the Langmuir isotherm is a good fit only for $\gamma(C)$ while it does not completely fit the relation of $\gamma(\Gamma)$. However, both F_1 and F_2 models, fit $\gamma(ln(C))$ and $\gamma(\Gamma)$ data profiles very well, with a slightly better fit for the F_2 model according to the insert in Fig. 2d. These fits are essential to determine the equilibrium parameters required to study the kinetics of surfactant mass transfer towards interfaces.

In subsection 2.2, the reference work of kinetics study by Ward and Tordai [35] will be discussed, along with other theoretical models to describe dynamics of surfactant mass transport.

2.2. Dynamics of surfactant mass transport

2.2.1. Mass transfer and adsorption kinetics equation

The mass transfer mechanism has been studied earlier in the literature by Milner et al. [60]. Assuming that the mass transfer in the bulk is governed by diffusion only and not by convection, the surface surfactant concentration Γ can be analytically calculated. At the instant t, Γ is expressed as follows [39]:

$$\Gamma(t) = 2c_0\sqrt{\frac{Dt}{\pi}} \tag{12}$$

with c_0 (mol/m^3) the initial bulk concentration and D (m^2/s) the diffusion coefficient defined by Fick's law. A more general form, considering back diffusion and the curvature of the interface can be written as follows [61]:

$$\Gamma(t) = 2\sqrt{\frac{D}{\pi}}\left[c_0\sqrt{t} - \int_0^{\sqrt{t}} c_s(t-\tau)d\sqrt{\tau}\right] \pm \frac{D}{R}\left[c_0 t + \int_0^t c_s(\tau)d\tau\right] \tag{13}$$

where c_s is the time dependent sub-surface concentration and R the characteristic radius of curvature of the interface. The - or + sign before the second term corresponds to a droplet or bubble, respectively.

The general form above takes into account the curvature of the interface. The impact of curvature on dynamic interfacial tension measurements has been subject to investigation, particularly by Reichert et al. [62] and Alvarez et al. [63]. These studies revealed discrepancies between the conventional planar model and a curved interface model within the context of diffusion-limited systems, when examining interfacial properties. This underscores the imperative of incorporating geometric considerations when applying theoretical frameworks to describe the mass transport of surfactant.

To compare this model with measurements of interfacial tension γ as a function of time, it is necessary to establish a link between coverage rate Γ and interfacial tension γ. This is done in two stages. Firstly, the adsorption dynamics equation will link coverage rate Γ and near-surface concentration c_s. Then, by considering the Gibbs equation of the interface given by Eq. 6, a link is established between surface tension, coverage rate and bulk concentration.

In 1969, Baret [64] proposed a theoretical model considering the adsorption/desorption kinetics at the interface. It is referred as the"-mixed-diffusion" or"mixed-kinetic" model. For a Langmuir mechanism,

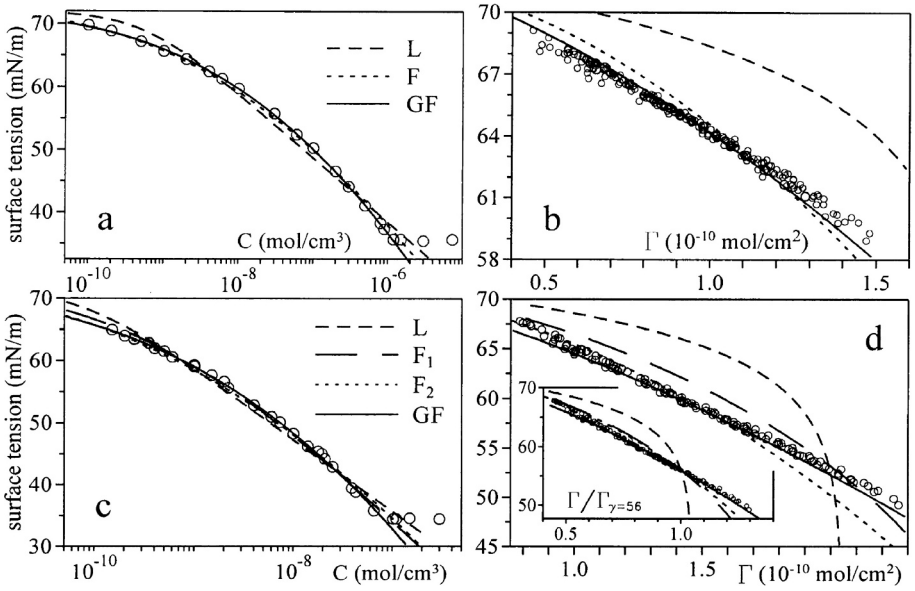

Fig. 2. Experimental data of (a and c) equilibrium surface tension $\gamma(C)$, (b and d) surface equation of state $\gamma(\Gamma)$, and model predictions using Langmuir (L), Frumkin (F_1 and F_2), and generalised Frumkin (GF) isotherms. L and F_1 were from the best-fit on $\gamma(ln(C))$ data; F_2 and GF were from the best-fit on both $\gamma(ln(C))$ and $\gamma(\Gamma)$ data. Parts a and b are for $C_{10}E_8$, and c and d are for $C_{12}E_8$. The insert in part d represents the relationship between surface tension and relative surface concentration. Reprinted with permission from Lin et al. [57]. Copyright 2003 American Chemical Society.

which means for an ideal and localised adsorbed layer, with equally partitioned adsorption sites, the rate equation is given by Eq. 2. For a Henry mechanism, so with $\frac{\Gamma}{\Gamma_\infty} \ll 1$, the rate equation reads:

$$\frac{d\Gamma}{dt} = k_a c(t) - k_d \Gamma \tag{14}$$

with k_a and k_d the adsorption and desorption constants related to the adsorption and desorption energies as explained before in subsection 2.1. Other more elaborate models for non ideal and mobile adsorbed layer have been built. The details of the calculations will not be given here but are completed in Baret's work [64]. One can also find in the literature the kinetics for Frumkin isotherm [36] where the interaction between solute molecules are considered during desorption using parameter A. The rate equation is:

$$\frac{d\Gamma}{dt} = k_a c(t) - k_d \Gamma exp\left(-A\left(\frac{\Gamma}{\Gamma_\infty}\right)\right) \tag{15}$$

Other theoretical frameworks based on the same ideas can be found in the literature [30,36,65]. At equilibrium, we find back the Frumkin adsorption model given by Eq. 9. When the link between the surface coverage Γ and the concentration at the interface is established, it is necessary to close the set of equations by linking the surface coverage and the interfacial tension. This is done by considering the Gibbs equation of the interface (Eq. 6) as before. The equilibrium Frumkin adsorption model is used to integrate the Gibbs equation and leads us to Eq. 11 with $n = 1$. When A = 0, corresponding to an ideal interface, the Langmuir model is recovered (Eq. 7). Note that these consideration can be extended to generalised Frumkin model (see Eq. 10 and Eq. 11).

2.2.2. *Diffusion controlled dynamics*

When the adsorption process is controlled solely by bulk diffusion, i.e. when there is an instantaneous equilibrium between the surface and the sub-surface, the surface concentration Γ can be obtained by solving Eq. 13, describing the mass transfer between sublayer and bulk, and Eq. 9 describing the equilibrium state between sublayer and interface. The surface tension is obtained through Eq. 11 with $n = 1$. This model is often coined in the literature as the Ward and Tordai model or as the"diffusion-controlled" model and can also be used to study liquid-liquid interfaces.

2.2.3. *Adsorption controlled dynamics*

When the adsorption process is controlled solely by surfactant adsorption, the surface concentration Γ can be obtained by solving, according to the adsorption model chosen, Eq. 2, Eq. 14 or Eq. 15, describing the kinetics between sublayer and interface assuming that the concentration in the sublayer is equal to the bulk concentration c_0. Knowing the temporal evolution of the surface coverage $\Gamma(t)$, the dynamic surface tension is obtained through Eq. 11 with $n = 1$. It should be stressed here that this last step is not rigorous. Indeed, the state law was obtained assuming an equilibrium between the volume and the adsorbed layer, an equilibrium which is not reached here. The assumption made is that a coverage degree corresponds to a surface tension value, even if equilibrium is not reached between the surface and the subphase.

2.2.4. *Mixed controlled dynamics*

In this situation, as before, the adsorption kinetics model (Eq. 2, Eq. 14 or Eq. 15) is solved, but to couple with the diffusion process occurring in the bulk, the concentration in the sublayer is determined overtime by Eq. 13. Then the dynamic surface tension $\gamma(t)$ is calculated from Eq. 11 with $n = 1$.

The current theoretical models cannot be used to fully describe surfactant mass transport mechanisms. The variety of models and assumptions one can find in the literature reflects the difficulties encountered by researchers in the field. One of the biggest challenges is to link the interfacial tension $\gamma(t)$ and surface coverage $\Gamma(t)$ at each instant time point. Usually, it is assumed that there is equilibrium between the surface and the subphase at each time, and Eq. 11 is used. Whether that is always rightfully done, is the question. Besides, empirical equations are sometimes used [66] to describe surfactant mass transport towards interfaces, which takes these descriptions outside the theoretical framework.

In this section, theoretical framework for studying dynamics of surfactant mass transport has been presented. In theory, it is possible to solve the equations for each case of dynamics: diffusion, adsorption or mixed controlled. However, it is often difficult to determine the driving process experimentally. As we will see in subsection 2.5, characteristic

time and length scales are used to predict the predominant dynamic regime for surfactant mass transport.

2.3. Concentrated surfactant solutions above the critical micellar concentration

Above the critical micellar concentration (*cmc*), surfactants are not only present as free molecules but also as micelles. Micelles do not absorb and are thus not surface-active entities of their own accord, but they do contribute to the supply of surface-active molecules through de-micellization. This keeps the free surfactant concentration in the system equal to the *cmc*, during the adsorption process of the free molecules. Many groups [67–69] have modeled micelles in solution to describe the dynamic surface tension process. These studies generally assume that adsorption kinetics are fast and that surface concentration at a given time is related to the molecular concentration at the same time near the surface according to e.g., a Langmuir-type isotherm. The time-dependent evolution of molecular concentration near the surface is governed by diffusion to the surface, with the de-micellization rate and micelle diffusion towards the surface which effectively reducing the diffusion distance that free molecules need to travel after de-micellization. Rillaerts and Joos [67] assume that micelles are in very large excess compared to monomers and neglect the diffusion of micelles towards the interface. This allows the surface-active molecules supply equation to be modified to:

$$\frac{\partial c}{\partial t} = D\frac{\partial^2 c}{\partial^2 z}c + k(cmc - c) \tag{16}$$

$$\frac{d\Gamma}{dt} = -D\frac{\partial c}{\partial z} \tag{17}$$

c is the free surfactant concentration, *cmc* is the critical micellar concentration, and k is the rate constant for de-micellization (in s^{-1}). $z = 0$ corresponds to the location of the flat interface. After tedious rewriting, and assuming that $c = cmc$ for z going to infinite this leads to:

$$\Gamma = D^{1/2}\left(\frac{Co}{k^{1/2}}\right)\left(\left(\frac{1}{2}+kt\right)erf(kt)^{1/2} + \frac{kt^{1/2}}{\pi}exp(-kt)\right) - \frac{2}{\pi^{1/2}}\int_0^{t^{1/2}} c_s(t-\tau)exp^{-k\tau}d\tau^{1/2} + 2k^{1/2}\int_0^{t^{1/2}} c_s(t-\tau)\tau^{1/2}erf\left(k\tau^{1/2}\right)d\tau^{1/2} \tag{18}$$

With c_s the concentration in the subsurface. Eq. 18 reduces to Eq. 13 when $k \to 0$ and when curvature is not considered (i.e., $R \to \infty$ in Eq. 13). By comparing surface tension data with the model, the authors show that this sequence describes the temporal evolution of surface tension. They found that de-micellization kinetic constants increase as a function of total surfactant concentration, which does not completely agree with the results of Krescheck et al. [70] results who use a different theoretical approach based on kinetics mechanisms that are also found in the work of Nyrkova et al. [71]. The simplified model proposed by Rillaerts and Joos [67] has been extended by Danov [68] and Noskov [69], who consider the diffusion of micelles towards the interface. They have performed numerical simulations to compare models and experimental data for SDS and SDP_2S and found them both in good agreement [68]. In the same framework, Glawdel and Ren [72] have suggested the following effective diffusion coefficient D_{eff} accounting for micelles contribution in surfactant mass transport:

$$D_{eff} = D(1+\alpha)\left(1+\alpha N_A^{-2/3}\right) \tag{19}$$

with $\alpha = c/cmc - 1$, c the surfactant concentration, *cmc* the micellar concentration and N_A the aggregation number of micelles. This effective coefficient can be used in some characteristic numbers for mass transport (see subsection 2.5 and subsubsection 4.1.3) when $c > cmc$.

Patist et al. [73] have highlighted the importance of micellar kinetics in droplet or bubble formation. Usually, the equilibrium between free surfactants and micelles is very fast but micellar kinetics can still be significant. For instance, Fainerman et al. [74] found that for Triton surfactants, the kinetics of micelles dissolution become significant at times greater than 10 *ms*. Beyond this time frame, they observed an increase in the rate of surfactant adsorption with increasing surfactant concentration (for $c > cmc$). This observation emphasizes the role of micelle dissolution in supplying free surfactant molecules.

2.4. Complex surface-active molecules

2.4.1. Proteins and polymers

Although proteins exhibit adsorption behaviour similar to that of surfactants, due to their specific structure, additional effects play a role such as denaturation or molecular reorientation which significantly alter the kinetics of adsorption [75]. Therefore, other equations have been built to describe their mass transport towards interfaces. Miller et al. [76] and Fainerman et al. [77] theoretically described the adsorption kinetics of proteins at liquid interface, based on the fact that proteins have different molar areas corresponding to different states of adsorption. The equation of state can be written as follows [76,77]:

$$-\frac{\Pi w_0}{RT} = ln(1-w\Gamma) + (w-w_0)\Gamma + a(w\Gamma)^2 \tag{20}$$

with w the average molar area (in m^2/mol), and a the intermolecular interaction parameter. The total adsorbed amount of protein in all n states is given by: $\Gamma = \sum_{i=1}^{n}\Gamma_i$ and the total surface coverage by: $\theta = w\Gamma = \sum_{i=1}^{n} w_i\Gamma_i$. The molar area varies from w_{max} at low surface coverage to w_{min} at high surface coverage. The adsorption isotherm as function of the molecular area and for each state (j) is given by:

$$b_j c = \frac{w\Gamma_j}{(1-w\Gamma)^{w_j/w}}exp\left(-2a\left(w_j/w\right)w\Gamma\right) \tag{21}$$

with b_j is the equilibrium constant of state j. Miller et al. [76] have shown that these equations combined with the Ward et Tordai theory (Eq. 13) describe the mass transport of proteins at low protein concentrations quite well. A similar approach has been used by Ramirez et al. [78] to study triblock copolymers by drop profile tensiometry, adsorbing at different molecular states (see Eq. 21). Besides, it has been observed experimentally that above a critical polymer concentration, aggregation takes place, and the surface pressure is significantly decreased. To consider this effect, an approximation of the surface pressure above this critical concentration can be expressed as:

$$\Pi = \Pi^*\left(1+\frac{\Gamma-\Gamma^*}{N_a\Gamma^*}\right) \tag{22}$$

with N_a the aggregation number, Π^* the surface pressure corresponding to the critical value of surface coverage Γ^*, above which aggregation of polymer at the interface is significant.

2.4.2. Polyelectrolytes and mixtures

Polyelectrolytes are polymers with many ionic sites which may lead to multi-layer formation and/or reorganization during the adsorption process. The adsorption mechanism, which is also chain length dependent, is different in the presence of surfactant molecules and polyelectrolyte /surfactant complexes, of which the effect is still not well understood. Mostly experimental studies have been performed with surface tension investigations being coupled to interfacial rheology [79–81]. Penfold et al. [81] have studied the mixture PEI/SDS at the air/water interface and highlighted the importance of the interaction between the polyelectrolytes and surfactants in the mixture. The stronger the interaction is, the more difficult it is to describe the behaviour at the interface. For weakly interacting nonionic polymer-surfactant mixtures, the adsorption process is mostly driven by the behaviour of the

surfactant molecules [81]. Novikova et al. [80] investigated the impact of the solution's ionic strength on the mass transport kinetics for PHMDAAC polyelectrolytes, and found them significantly enhanced. Surface elasticity measurements have also been performed to investigate the different mechanisms occurring at the interface.

For a comprehensive overview, we recommend the review of Aidarova et al. [79] that includes analysis on interfacial tension, rheology, electrokinetic properties and hydrodynamic parameters of polyelectrolytes and polyelectrolyte/surfactant mixtures.

2.4.3. Asphaltenes

Asphaltenes are constituents of crude oil of which the adsorption properties exhibit similarities with proteins. The Yen-Mullins model [82] that is used in the oil industry, describes the molecular structures of asphaltenes in several solvents and crude oil. Langevin and Argillier [83] reviewed the interfacial properties of asphaltenes and found that at low concentration, asphaltenes adsorb as molecular layers and at higher concentration as aggregates. It is difficult to capture this in a theoretical model but Langevin and Argillier [83] believe that the interfacial tension varies through a superposition of exponential decays, instead of a simple exponential. The complex surface-active molecules mentioned in this section exhibit different mass transport kinetics and adsorption mechanisms mostly due to their molecular structures, and possible reorganization at the interface, for which no general model is yet available.

2.5. Characteristic time and length scales

To identify the limiting mechanism under specific experimental conditions and studied systems, it is crucial to define characteristic time and length scales associated with these mechanisms. The simplest assumption made is a planar interface and the diffusive time scale associated with diffusion-controlled mass-transfer is defined as: $\tau_D = h_p^2/D$. h_p is the characteristic length scale for diffusion onto a planar interface and can be expressed as: $h_p = \Gamma_{eq}/c_0$ with c_0 the bulk concentration and Γ_{eq} the concentration of surfactant at the interface at equilibrium. It has been shown by Ferri et al. [84] that for high enough bulk concentrations, this time scale is indeed relevant for surfactant mass transport limited by diffusion.

In 2016, Riechers et al. [15] have studied adsorption kinetics to better understand emulsions lifetimes with a microfluidic method, by measuring the adsorption kinetics of carboxylic acid surfactant in a droplet. The authors have discussed the regimes of surfactant mass transport: one diffusion controlled regime, and the other one only limited by a Langmuir process of mass transport at the interface. To determine the limiting mechanism, they have defined characteristic timescales and showed that for a sphere, the diffusion timescale R^2/D should be compared to the one given by a Langmuir model $D/\left(k_{ads}^2.\Gamma_\infty^2\right)$ where D is the diffusion coefficient, Γ_∞ the maximal interfacial coverage and k_{ads} the adsorption rate. Following the work of Pan et al. [85] and Jin et al. [86], a new length scale for spherical systems such as droplets and bubbles to determine the adsorption regime is identified. Riechers et al. [15] proposed a study based on scaling arguments to separate diffusion limited and kinetic limited regimes, where $R^\star$ is the cutoff radius below which diffusion is always negligible. For a kinetic limited system described by a Langmuir isotherm, the characteristic time scale obtained by resolving Eq. 2 is the following: $t_k = \frac{1}{k_a c + k_d}$ with k_a and k_d respectively adsorption and desorption constants. When the two time scales are equal (i.e $\tau_D = t_k$), Jin et al. [86] noted an intrinsic length scale $R^\star$ defined as:

$$R^\star = \frac{D}{\Gamma_\infty k_{ads}} \tag{23}$$

Fig. 3, taken from Riechers et al. [15] shows the different scaling for early adsorption kinetics. The surface coverage Γ as a function of time on log scale is displayed, for a purely diffusive system for a flat interface where $\Gamma \propto \sqrt{t}$ and for a sphere with $\Gamma \propto t^{3/2}$. For Langmuir-type kinetics, a linear relation is found between the surface coverage and time. The characteristic time scales are displayed in the x-axis where the cutoff time scale R^2/D marks the transition of the kinetic and diffusive regimes for a spherical geometry. In their experiments, Riechers et al. [15] took advantage of a system of small droplets where diffusion is much faster than adsorption. Their study system is an acidic surfactant (PFPE with a carboxylic head group; KrytoxFSL; DuPont). When a surfactant molecule adsorbs, it produces an hydronium ion. By following the evolution of pH over time at very long time i.e. when the surfactant coverage is close to equilibrium, they were able to measure the adsorption constant of surfactant molecules. They have shown that the systems studied follow a kinetic-limited model, as a second-order Langmuir process.

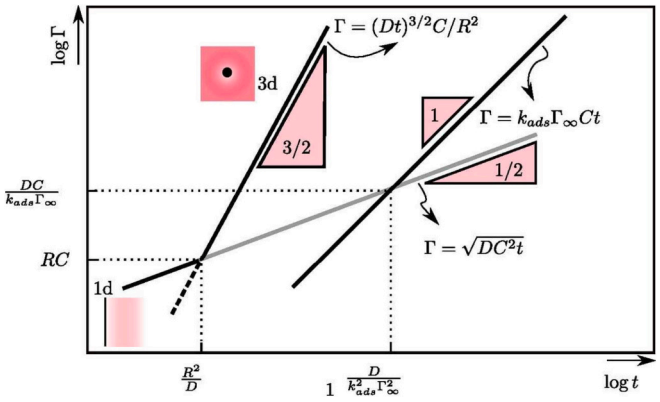

Fig. 3. Scaling laws for the early time adsorption kinetics. The determination of the cutoff radius is shown. When the interfacial coverage is limited at an early stage by a diffusive process, a square root dependence with time is obtained for a flat interface. For a sphere, the power law has a 3/2 exponent. In the kinetic regime, a linear dependence is obtained for a Langmuir-type kinetics.The crossovers between the different regimes reveal that for sufficiently small droplets, the mass transfer is never diffusion-limited. - From Riechers et al. [15].

A similar study has been carried by Alvarez et al. [87] where they considered curvature of interfaces. A new diffusive length scale for spherical geometry has been calculated taking into account the bubble radius b, $h_s = b\left(\left(\frac{3h_p}{b}+1\right)^{1/3} - 1\right)$ where h_p is the classical diffusive length scale for a flat interface, defined earlier. Thus, by scaling argument, the diffusive time scale becomes: $t_{D,s} = \frac{\left(h_s^3 h_p\right)^{1/2}}{D}$. The cutoff radius between diffusion and adsorption controlled regimes is the same as given by [15,85,86], $R_{DK} = R^\star$. To take into account the spherical geometry, Alvarez et al. [87] calculated a new critical radius as R_{crit} and showed this new characteristic length depends on the bulk concentration and experimental conditions as follows:

$$\frac{R_{crit}}{R_{DK}} = \frac{2}{\sqrt{12 - 3q^2} - 3q} \tag{24}$$

with $q = \left(R_{DK}/h_p\right)^{1/3}$. They have performed surface tension measurements with bubbles of radii from 17μm to 150μm with a microtensiometer. Fig. 4 shows the influence of bubble radius for systems that follow a Langmuirian kinetic exchange at the interface. On this graph, large droplet or bubble radii are at the top left, while small droplet or bubble radii are at the bottom right. When bubble radius decreases, mass transport dynamics becomes more kinetic limited. It also shows that concentration does influence the surfactant kinetics which is in agreement with observation of a shift from diffusion-limited to kinetics-limited in different systems of the literature [49,85,88].

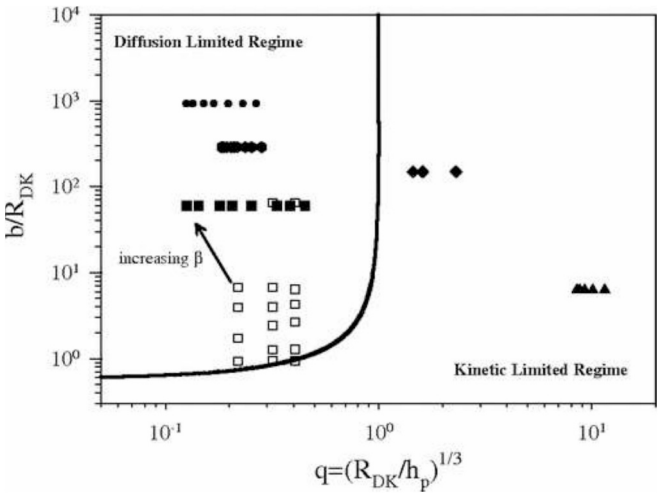

Fig. 4. The effect of bubble radius and concentration on the governing transport of a soluble adsorbing species following Langmuirian kinetics. The line corresponds to equality of the diffusion time scale and the kinetic time scale. Diffusion-limited dynamics exist far to the left of the line and kinetic-limited dynamics exist far to the right of the line. The points correspond to data extracted from literature (filled symbols) or conducted with varying bubble size (open symbols). ▲ butanol; ◆ hexanol; ● decanol; ■ $C_{12}E_8(C_{bulk})$ and $C_{12}E_8(b)$. Here, β is the adsorption constant referred as k_a in our text ($\beta = k_a$). Reprinted with permission from Alvarez et al. [63]. Copyright 2010 by the American Physical Society.

This study shows that when small droplets are formed, the evolution of interfacial tension over time will be driven by surfactant adsorption kinetics and not by material transfer from the volume to the interface. In what follows, we shall see that microfluidic techniques can be used to generate drops of micronic size. We anticipate that these techniques will enable us to measure adsorption kinetics to the detriment of knowledge of diffusion parameters.

3. Dynamic interfacial tension measurements to study surfactant mass transfer towards the interface

In the previous part, theoretical models describing surfactant repartition at equilibrium and through time have been reviewed. The systems under study can be dominated by either diffusion, adsorption or a mixed-diffusion process. Dynamic interfacial tension measurements have been widely performed in the literature. Depending on the experimental conditions, these experiments can be used to determine either the diffusion coefficients of the surfactant in the solution (subsection 3.1), or the kinetic constants involved in the reaction at the surface (subsection 3.2). These approaches require the use of thermodynamic models such as those described in the previous section. At the end of this section, Table 1 provides the equilibrium data from the literature reviewed and Table 2 provides diffusion characteristic time and length scales from the studies analysed in this part.

3.1. Diffusion limited systems and experimental conditions for determining diffusion parameters

This section aims to demonstrate how the diffusion coefficients for surfactants mass transport towards the surface can be measured, and how the surface tension curve can be modeled. To do this, we need to consider conditions where adsorption kinetics at the surface are rapid, and where the measurement method favors adsorption kinetics over diffusion mass transfer. This means working on large droplets, according to the radius criterion (see Eq. 23). First, we will show some measurements that fall within this field, then we will illustrate cases where adsorption kinetics are too slow and become the mechanism governing the temporal evolution of interfacial tension.

In 2020, Qazi et al. [89] have studied the dynamic surface tension of ionic CTAB and nonionic Tween 80 surfactant solutions. The authors have determined the surface excess concentration Γ below the CMC, with the Gibbs adsorption isotherm given by Eq. 6. The maximum bubble pressure measurements reach a time scale from 1 s to 10^3 s. The characteristic diffusion time is defined by the time for the surface

Table 1
Equilibrium data from the literature. Γ_∞ is the maximum surface coverage expressed in mol per surface unit.

Surfactant	Concentration range	Interface nature	Measurement method	Isotherm	Γ_∞ (mol/m^2)	Reference
Triton X-45	(0.2–50) $\times 10^{-6}$ mol/L	aqueous solution / air or hexane	Bubble/drop profile; Maximum bubble/drop pressure	Frumkin	–	Fainerman et al. [94,96]
Triton X-100	(0.2–50)$\times 10^{-6}$ mol/L	aqueous solution / air or hexane	Bubble/drop profile	Frumkin	–	Fainerman et al. [94,96]
Triton X-165	(0.1–50) $\times 10^{-6}$ mol/L	aqueous solution / air or hexane	Bubble/drop profile	Reorientation model	–	Fainerman et al. [94,96]
Triton X-405	(0.01–50) $\times 10^{-6}$ mol/L	aqueous solution / air or hexane	Bubble/drop profile	Reorientation model	–	Fainerman et al. [94,96]
$C_{12}E_8$	6.25 $\times 10^{-6}$ mol/L	aqueous solution / air	Pendant bubble	Frumkin	5.3×10^{-6}	Reichert et al. [62]
				Langmuir	2.1×10^{-6}	
$C_{12}E_8$	1.5 $\times 10^{-7}$ mol/L	aqueous solution / air	Pendant bubble	Frumkin F_1	2.7×10^{-6}	Lin et al. [57]
				Frumkin F_2	3.5×10^{-6}	
$C_{12}E_4$	1.5 $\times 10^{-5}$ mol/L	aqueous solution / air	Pendant bubble	Langmuir	3.9×10^{-6}	Lin et al. [57]
				Frumkin F_2	4.6×10^{-6}	
				Generalised Frumkin	6.6×10^{-6}	
$C_{10}E_4$	1.3 $\times 10^{-5}$ mol/L	aqueous solution / air	Pendant bubble	Langmuir	3.0×10^{-6}	Lin et al. [57]
				Frumkin F_1	3.8×10^{-6}	
				Frumkin F_2	4.6×10^{-6}	
$C_{12}E_6$	(0.01; 0.04; 0.2) $\times 10^{-4}$ $mol/L(<cmc)$	aqueous solution / air	Pendant bubble; bubble compression	Gibbs isotherm	3×10^{-6}	He et al. [92]
CTAB	(0.03; 0.1; 0.2) $\times 10^{-4}$ $mol/L(<cmc)$	aqueous solution / air	Pendant bubble; bubble compression	Gibbs isotherm	3.5×10^{-6}	He et al. [92]
CTAB	(0.2–1) $\times 10^{-3}$ $mol/L(<cmc)$	aqueous solution / air	Maximum bubble pressure	Gibbs isotherm	–	Qazi et al. [89]
Tween 80	(0.8–1) $\times 10^{-4}$ mol/L	aqueous solution / air	Maximum bubble pressure	Gibbs isotherm	8.5×10^{-7}	Qazi et al. [89]
$C_{13}DMPO$	1 $\times 10^{-8}$ - 1 $\times 10^{-7}$ mol/L	aqueous solution / air or hexane	Maximum bubble pressure	Langmuir	9.83×10^{-6}	Ferrari et al. [105]

Table 2
Dynamic properties for diffusion-limited systems. Diffusion length and time scales are not always directly given by the authors so they have been calculated from other characteristic parameters given in the articles, according to the geometry assumptions made.

Surfactant	Measurement method	Measurement time scale	Geometry	Diffusion length scale h (m)	Diffusion time scale τ_D (s)	Diffusion coefficient D (m^2/s)	Reference
Triton X-45	Bubble/drop profile; Maximum bubble/drop pressure	0.05–200 s	Planar	–	–	(1.5–3.0) $\times 10^{-10}$	Fainerman et al. [94,96]
Triton X-100	Bubble/drop profile	0.05–200	Planar	–	–	–	Fainerman et al. [94,96]
Triton X-165	Bubble/drop profile	–	Planar	–	–	(1.3–1.8) $\times 10^{-9}$	Fainerman et al. [94,96]
Triton X-405	Bubble/drop profile	–	Planar	–	–	–	Fainerman et al. [94,96]
$C_{12}E_8$	Pendant bubble	1 - 10^4	$R = 1$ mm	5.25×10^{-4}	9.21×10^2	3.8×10^{-10}	Reichert et al. [62]
$C_{12}E_8$	Pendant bubble	1 - 10^4	R = 1 mm	2.5×10^{-3}	$1.35 - 1.90 \times 10^4$	(7.8–11) $\times 10^{-10}$	Lin et al. [57]
$C_{12}E_4$	Pendant bubble	1 s - 10^4 s	R = 1 mm	2.12×10^{-4}	76.5	6.5×10^{-10}	Lin et al. [57]
$C_{10}E_4$	Pendant bubble	1 s - 10^4 s	R = 1 mm	1.92×10^{-4}	62.0	6.5×10^{-10}	Lin et al. [57]
$C_{12}E_6$	Pendant bubble; bubble compression	< 100 s	Planar	7.50×10^{-4}	1.48×10^3	$(3.8 \pm 0.5) \times 10^{-10}$	He et al. [92]
CTAB	Pendant bubble; bubble compression	< 100 s	Planar	3.52×10^2	3.25×10^{-4}	3.0×10^{-10}	He et al. [92]
CTAB	Maximum bubble pressure	> 1 s	Planar	1.75×10^{-4}	–	–	Qazi et al. [89]
Tween 80	Maximum bubble pressure	> 1 s	Planar	1.06×10^{-5}	–	–	Qazi et al. [89]
$C_{13}DMPO$	Maximum bubble pressure	–	Planar	9.83×10^{-2}	4.8×10^7	2.0×10^{-10}	Ferrari et al. [105]

tension γ to reach half of its equilibrium value [89]. For surfactant solutions exhibiting rapid surface tension decay (in the order of tens of milliseconds), Qazi et al. [89] performed measurements with the Kruss Maximum Bubble pressure (BP50) tensiometer. This instrument allowed measurements in the time range of 14 milliseconds to 16 s. According to Ward and Tordai theory [39], the characteristic diffusion time should scale with the square of the bulk concentration. Experimental data from Qazi et al. [89], for CTAB solutions, are in agreement with Ward and Tordai theory, since the characteristic time follows the diffusion scaling for diluted solutions (concentrations below the CMC). Thus, the authors have proven that for the range of concentrations studied below the CMC, from 2×10^{-4} to 10^{-3} mol/L for CTAB and from 8×10^{-5} to 10^{-4} mol/L for Tween 80, the adsorption mechanism was diffusion-limited and in good agreement with the theoretical models. Qazi et al. [89] also studied the influence of salt concentration in CTAB systems, and ruled out the existence of a possible adsorption barrier. In a novel approach, the authors used sum-frequency generation (SFG) spectroscopy to probe the orientation of adsorbed molecules at interfaces and perform surface excess measurements. Thanks to these techniques, Qazi et al. [89] were able to show that the adsorption barrier in these ionic systems was very low, as the counter ions molecules condensed on the CTAB molecules adsorbed on the surface. This study clearly shows the experimental conditions required to measure equilibrium isotherms and diffusion constants accurately: use of large droplets and surfactant molecules with low adsorption barriers.

Another way of making measurements within the framework of the diffusion hypothesis is to use a compression bubble method, similar to a Langmuir trough. The experimental protocol is described in detail elsewhere [49,90–92] and relies on the surface tension and surface area measured during the compression of the bubble. This method, which does not require the use of isotherms and where the interfacial tension is directly linked to the excess concentration, is a real breakthrough. From a freshly formed bubble, after a time during which it evolves at a constant surface area, the authors compress the bubble until γ_{eq} is reached. Since the compression time is much faster than the desorption of the molecules, during the whole process, and at each time, $\Gamma A = \Gamma_{eq} A_{eq}$. By monitoring the surface area during the compression process, it is possible to directly evaluate the ratio Γ/Γ_{eq} as a function of time. By also measuring interfacial tension, the equation of state can be deduced, without the use of Gibbs relation (Eq. 6). With this method, He et al. [92] have studied two systems: solutions of *CTAB*/*NaBr* at concentrations ranging from $3 \times 10^{-6} mol.L^{-1}$ to $10 \times 10^{-6} mol.L^{-1}$ and solutions of $C_{12}E_6$ at concentration ranging from $1 \times 10^{-6} mol.L^{-1}$ to $20 \times 10^{-6} mol.L^{-1}$. A diffusion-controlled mass transport mechanism is assumed and according to Ward and Tordai theory [39], at short times and a bubble radius bigger than the adsorption length, the ratio of surface excess concentration can be written as:

$$\frac{\Gamma(t)}{\Gamma_{eq}} = 2\sqrt{\frac{D}{\pi}}K \tag{25}$$

with $K = \left(C_{bulk}/\Gamma_{eq}\right)\sqrt{t}$. Fig. 5 shows that the experimental data are in good agreement with the theory, confirming both systems are limited by diffusion in these experimental conditions. The method was also verified by comparing their results with the ones given by the Gibbs equation.

From these data and curve fitting, the calculated diffusion coefficients are found to be of $(3.8 \pm 0.6) \times 10^{-10} m^2/s$ for $C_{12}E_6$ and of $(3.0 \pm 0.5) \times 10^{-10} m^2/s$ for CTAB, comparable with the literature.

While this study shows that it is possible to study diffusion limited systems without the use of theoretical equations, classical methods such as pendant drop/bubble or maximum bubble pressure techniques have been successfully used in the literature to study diffusion process. For instance, using dynamic tension measurements based on the maximum bubble pressure technique, Miller et al. [76] were able to measure the diffusion coefficient of beta-casein molecules. In fact, at low concentrations, dynamics is governed by the diffusion mechanism, whereas at high protein concentrations, this is only the case in the initial phase, at short times. The effective diffusion coefficients correspond fairly well to literature data. Adsorption values calculated from dynamic surface tension data agree very well with the equilibrium adsorption model used. Similar conclusions were reached by Ybert et al. [93] with bovine serum albumin (BSA) proteins.

The non ionic C_iE_j surfactants have also been well studied in the literature [55,88], and particularly in two main articles by Lin et al. [57,58]. It has been demonstrated [55,88] that for dilute solutions, nonionic polyoxyethylene surfactants C_iE_j mass-transfer onto a freshly created interface is controlled by diffusion, while at higher concentrations, a shift to a mixed-diffusion mechanism has been reported [55,88]. In the concentration ranges where the mass-transfer of these surfactants is limited only by diffusion, Lin et al. [57,58] have studied equilibrium and dynamic interfacial properties, with pendant bubble measurements. For dilute solutions they were able to measure the diffusion coefficient

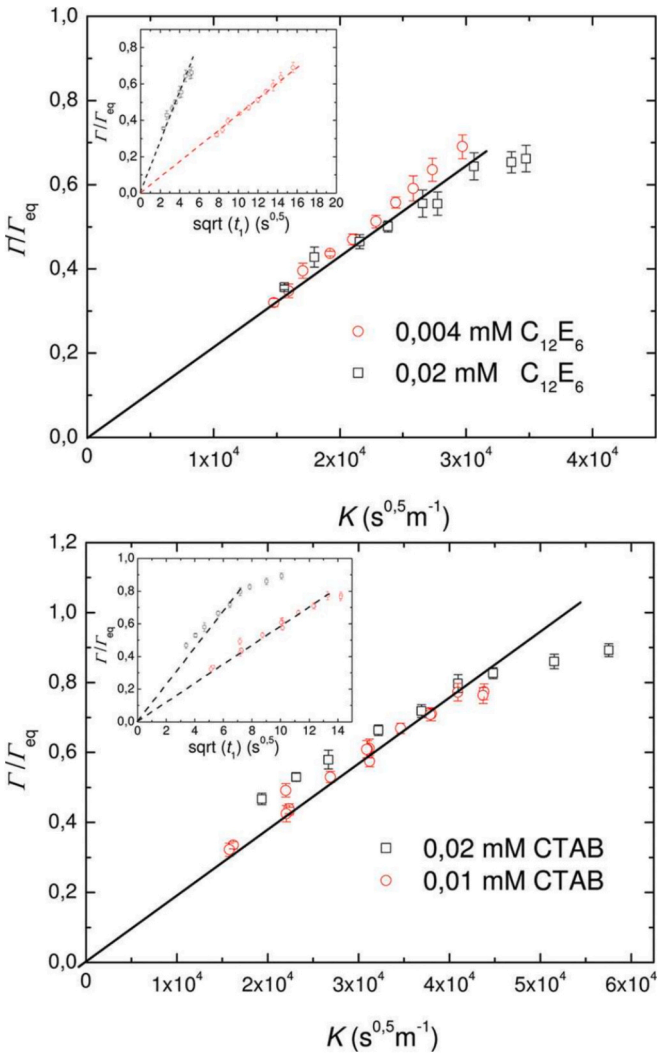

Fig. 5. Surface excess ratio Γ/Γ_{eq} as a function of $K = (C_b/\Gamma_{eq})(t_1)^{1/2}$ for two surfactants at different concentrations. The insert shows the Γ/Γ_{eq} as a function of $(t_1)^{1/2}$. Reprinted with permission from He et al. [92]. Copyright 2012 American Chemical Society.

of the molecules. They have confirmed the previous observations of the shift from one diffusive regime to another mixed one and, as explained in section 2, the isotherm choice is proven to be determinant when studying mass-transfer of surfactants.

The above studies are ideal studies, carried out under conditions that allow adsorption mechanisms to be separated. The dynamics is limited by diffusion in the situation where a low energy adsorption barrier exist, where measurements performed at short time, in dilute solutions and with large bubbles in the maximum bubble pressure methods are used. As we shall see below, these conditions are not always met. In the examples that follow, experimental conditions are often less than ideal, making it difficult to access diffusion coefficients precisely.

3.2. Adsorption limited systems and experimental conditions for determining adsorption parameters

In their pioneering studies, Ward and Tordai [39] came up against difficulties to determine diffusion coefficients in their systems. The theoretical article presenting their founding model is accompanied by experiments using the maximum bubble pressure technique. They have tested their theory on several systems such as alcohol solutions and palmitic acids. In order to validate their model, diffusion coefficients D were calculated and compared with the literature. They have found that for most of the systems studied, the diffusion coefficient's values were below the ones encountered in the literature. Ward and Tordai [39] concluded that the processes were not only determined by diffusion and they suggested the existence of an activation barrier to explain the deviation from diffusion theory. The existence of adsorption barriers has been repeatedly reported in studies that measure surface tension by maximum bubble pressure. In the following, we will show that high surfactant concentrations make it impossible to measure the diffusion coefficient D, leaving the possibility of measuring kinetic constants indirectly.

One of the most studied family of non ionic surfactants is Triton, especially for Triton X-100; many parameters have been investigated such as interfacial tension at air/water or oil/water interfaces or influence of temperature [46]. In fact, one of the most accomplished investigations of mass transfer mechanism encountered can be found in Fainerman et al. [94] work. The dynamic interfacial tension is measured with the droplet or bubble profile analysis tensiometers and the model used is derived from diffusion theory, generalised to a system with surfactant initially present in both phases. Their calculations are inspired by Ward and Tordai [39] and the authors completed their work with numerical modeling [95]. Two models are compared with the experimental measurement of the dynamic interfacial tension as a function of time: the Frumkin one and the approximate reorientation model. The latter assumes that two orientations of adsorbed surfactant molecules exist at the surface, with different molar areas.

The reorientation model is a model that has been used to describe adsorption of proteins [76]. In this paper, the authors have resumed the Eq. 20 and Eq. 21 with two orientations with molar areas w_1 and w_2.

They have tested the adequacy of the models for four types of Tritons, in order of increasing polar chain length: X-45, X-100, X-165 and X-405 within a wide time range from 10^{-4} s to 10^4 s. For the first Tritons, experimental results agree with the Frumkin model, validating the diffusion-controlled mechanism throughout the whole time range. However, for the Tritons X-165 and X-405, the dynamics were not in agreement with the classical Frumkin model, so the experimental data were compared with the approximate reorientation model, as displayed in Fig. 6.

For Tritons surfactants, an increase in surface activity was observed for molecules of larger molar area of oxyethyl groups [95]. These authors [96] found $w_2 = 16 \times 10^5\ mol/m^2$ for the Triton X-405, while

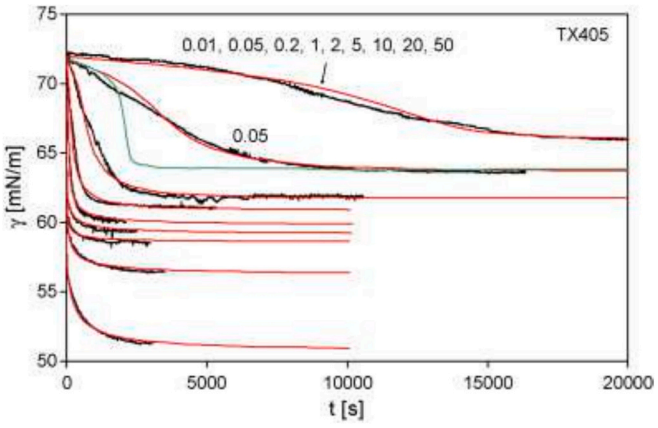

Fig. 6. Dynamic surface tensions of TX405 solutions measured by the emerging bubble profile method at different concentrations (in μmol/L); black curves are experimental data; red curves are calculations from the reorientation model with correction; green curves are calculations from the reorientation model without corrected parameter. Reprinted from Fainerman et al. [96]. Copyright 2009 with permission from Elsevier. (For interpretation of the references to colour in this figure legend, the reader is referred to the web version of this article.)

Miller et al. [97] found a typical value of $w_2 = 10^7\ mol/m^2$ for globular proteins. These differences originate from the size and nature of the molecules: proteins are much larger than surfactants, and the reorientation possibilities are probably higher. The reorientation model agrees well with experimental data and provides information about the different states of adsorption. For more details on the construction of the theoretical model, the reader may refer to the series of articles from Fainerman et al. [95,96,98].

This model takes into account the possibility of asymmetric surfactant adsorption in two or more states [99,100], which adds another parameter to the classical Frumkin model. Apparent diffusion coefficients were calculated and found to be influenced by the concentration in the bulk, which could indicate that mass transfer is not driven by diffusion only. However, the theoretical models used are based on equations for diffusion-controlled surfactant mass transfer and are in good agreement with experimental data if one takes the appropriate diffusion coefficient. The difficulties encountered with the determination of diffusion coefficients can also be explained by the non ideality of the solutions. Considering a mixture of surfactants with different ethylene oxide groups, would surely improve the model. This paper also highlights the importance of the measurement method on the time scales since for the Triton X-100, the maximum bubble pressure method is suitable for time ranges below 10 s whereas the pendant drop profile method completes the other one by measuring surface tensions above 10 s. The comparison of these models was also discussed with the case of ethoxylated alcohols by the same group in 2003 [101].

As mentioned earlier in the previous section (subsection 3.1), the C_iE_j surfactants are a good example of systems that cannot be described by the same limiting mechanism for mass transport, for the whole concentration range. In fact, Chang et al. [55] have studied the mass-transfer of $C_{10}E_8$ surfactants at different concentrations and confirmed the shift from diffusion-controlled to mixed-diffusion mechanism by comparing numerical simulations with experimental data. Fig. 7 displays the results obtained by them. All the curves are obtained using the generalised Frumkin model and simulations have been performed for different adsorption rate constants. In Fig. 7, experimental data are in good agreement with the diffusion controlled model. These data have been obtained with a dilute solution. When the bulk concentration increases, as seen in the last two plots (for example for $C_0 = 4.0 \times 10^{-9}$ mol/cm^3 and $C_0 = 1.0 \times 10^{-8}\ mol/cm^3$ in Fig. 7b,c), the diffusion curves are deflected from the experimental points and the mixed-controlled model is a better fit. This work on $C_{10}E_8$ from Chang et al. [55] is similar to the study of $C_{12}E_8$ surfactant done by Lin et al. [58,102]. They have used the same pendant drop method to study dynamic surface tension of this surfactant and also found a shift from diffusion to mixed-kinetic controlled mass-transfer at higher concentrations. Both works highlighted the dependency of adsorption/desorption rates on bulk concentration and they deduced that the Frumkin and the generalised Frumkin models describe adsorption mechanisms better [55,58,85,102,103].

We anticipate that although this work is exemplary in terms of measurement precision, the difference between the theoretical curves, which assumes that kinetics are limited by diffusion or adsorption, is still very small. It seems necessary to find techniques that can better separate the two mechanisms.

Similar conclusions were reached by Lee et al. [49] with bubble compression technique, where adsorption and desorption processes have been studied independently. They have shown that desorption is always mixed-diffusion controlled [103] while adsorption process can be driven by different mechanisms according to the surfactant nature: diffusion-controlled for $C_{14}E_8$ and mixed-diffusion control $C_{10}E_8$ and $C_{12}E_8$. The generalised Frumkin model is also found to describe the equation of state ($\Gamma(\gamma)$) and equilibrium parameters more accurately.

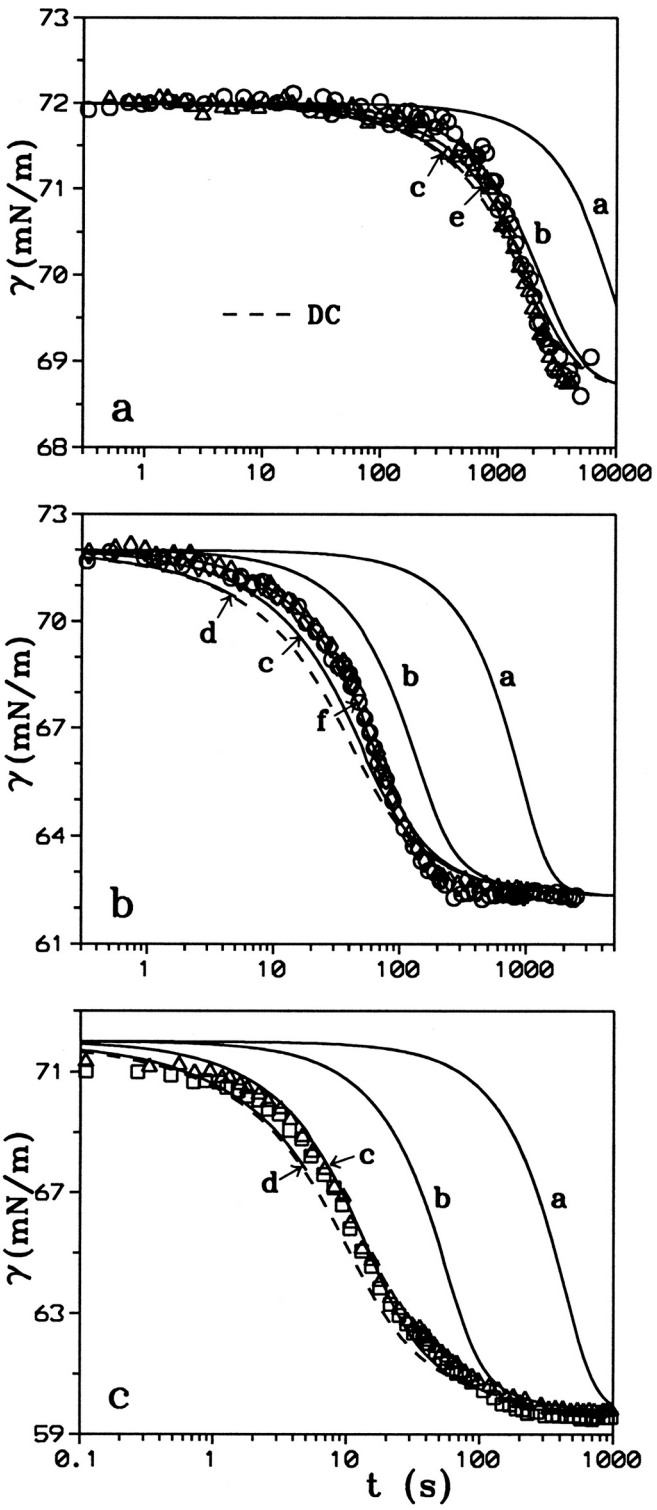

Fig. 7. Dynamic surface tension (mN/m) for adsorption of $C_{10}E_8$ and theoretical predictions of mixed controlled adsorption and diffusion controlled mechanism for different adsorption rate constants ($a = 10^5, b = 10^6, c = 10^7, d = 10^8, e = 2.5 \times 10^6$ and $f = 5 \times 10^6 cm^3/(mol.s)$) calculated from the generalised Frumkin model. $C_0 = 0.20(a), 4.0(b)$ and $10.0(c)$ $[\times 10^{-9} mol/cm^3]$. Dashed lines denote the diffusion-limited curves with $D = 6.5 \times 10^{-10} m^2/s$. Reprinted with permission from Chang et al. [55]. Copyright 1998, American Chemical Society.

For these C_iE_j surfactants, the shift to mixed-kinetic controlled mechanism at higher concentrations may also be explained by the presence of micelles. In 2000, Zhmud et al. [104] have highlighted the difficulties to have a general accurate model for mass transport. They have studied a series of C_iE_6- type surfactants for aqueous solutions at concentration from 0.1 CMC to 5 CMC at short time, below 1 s. For the concentrations above the CMC, it is necessary to consider the heterogeneity of the solution where both monomers and micelles are present, each having a different behaviour towards the interface. The authors have chosen Fainerman's [99] theory, well describing the micelle kinetics by adding to the classical diffusion equations a source term allowing micellar decay. Zhmud et al. [104] have completed the model by redefining the source to consider the formation of micelles in the system. Similarly to Fainerman et al. [96] studies, a dependency of diffusion coefficient with concentration is observed, which could be explained by interconversion and rearrangement of several species at the air/water interface. However, the values obtained with the Fainerman's [99] model are not consistent with independent experimental values [104]. The authors account these discrepancies by pointing out the neglect of polydispersity of micelles. The observations made and the deviation from the diffusion theory have been confirmed by Lin et al. [58] with the same surfactants but they explained them by the shift to mixed-diffusion control process.

The analysis that can be made from this review of the literature is that maximum bubble measurement and pendant drop profile methods do not provide simple access to kinetic parameters. Although diffusion is often the main mechanism responsible for temporal evolution, the latter is, in many cases (high concentration, long time scales, small surface areas, molecular orientation), influenced by surface adsorption mechanisms. The two mass transfer mechanisms become difficult to distinguish. In what follows, we will see that microfluidic techniques can, in some cases, circumvent this obstacle and hold great promise.

4. Study of interfacial properties in microfluidics

In the previous sections, studies of dynamic interfacial properties with conventional tensiometers have been reviewed. From the analysis of the literature, we have seen that it remains difficult to extract kinetic parameters accurately [106] and that diffusion cannot always be considered as the only limiting step during surfactant mass transport [55,58,104]. Only the study by Riechers et al. [15] using a very special system has enabled a clear measurement of an adsorption kinetic constant. This study stood out by employing very small droplets (50 μm) made using a microfluidic device. Microfluidics is a technology that has been developing for around thirty years, enabling fluids to be manipulated on micron scales [107,108]. It owes its rise and democratisation to the development of microfabrication techniques [109,110].

In the last part of this review, we will start by presenting microfluidic devices designed to measure interfacial parameters. The measurements require droplet or bubble formation and you can find different reviews about this topic in the literature [111–115]. They also require the measurement of a quantity sensitive to interfacial tension. The measurements are based on different physical phenomena: capillary pressure [116], droplet deformation [66], droplet size [87], hydrodynamics transition [117,118]. The subsection 4.1 reviews the different microfluidic devices that perform interfacial tension measurements, and the subsection 4.2 gives examples of studies in which interfacial tension measurements are performed with microfluidic devices to extract kinetic parameters.

4.1. Microfluidic devices to measure interfacial parameters

In this section, we will concentrate on new devices suited to understand surfactant mass transport, through interfacial tension measurements. The methods, advantages and limits of the devices regarding the determination of interfacial properties are compared. Besides, the time allotted for surfactant mass transport towards interface before measuring the interfacial tension is specified. The definition of this time is of prime importance to plot kinetics curves ($\gamma = f(t)$) and interpret them properly with kinetics models. A concise summary of the discussion can be found in Table 3. We will conclude this section by showing that the use of such device paves the road for adsorption constant rate measurements.

4.1.1. Dynamic interfacial tension measurements based on Laplace pressure

Alvarez et al. [87,106] have built a microtensiometer based on hydrostatic pressure equilibrium and radius of the droplet/bubble formed. A capillary is immersed in a semi-infinite surfactant solution. The bubble is formed with a pressure controller. The dynamic interfacial tension is calculated from the Laplace pressure as follows:

$$\gamma(t) = \frac{1}{2}\Delta P(t).R(t) \tag{26}$$

The pressure drop is measured between the tip and the head of the capillary. To measure the dynamic surface tension, air is injected through the capillary to create a bubble that is held at constant pressure and its radius is measured through time [106].

Besides, as mentioned in section 2, this article provides an interesting length scale to compare diffusion to kinetic limited regimes (Fig. 3 and Fig. 4), for a Langmuirian system. With this scaling, they have compared the microtensiometer to the conventional pendant drop tensiometer, and the operating diagram for both devices (Fig. 8). The shaded regions correspond to the experimental regimes and for the pendant drop, it is clear that, for diluted solutions, the kinetic regime cannot be observed. In fact, it is possible to reach this regime with the pendant drop method only for a system with a kinetic adsorption constant $\beta = k_a < 0.1$ $m^3/(mol.s)$, whereas for the microtensiometer, the kinetic regime can be observed more easily. With their device, the authors have been able to study interfacial properties of $C_{12}E_8$ surfactant as we have already mentioned before in a previous section [87,106], and have been able to approach kinetic-limited regime for $C_{12}E_8$ and $C_{14}E_8$ at the air/water interface.

The Laplace pressure equation has also been used in a recent work from Liang et al. [119], in which they developed a microfluidic tool to study the adsorption kinetics of classical nonionic surfactants (Tween 20, Triton X-100, Brij 58 and Brij 56). The tensiometer is a co-flow device as shown in Fig. 9, equipped with pressure sensors. The interfacial tension is determined using the Laplace pressure equation, and is as follows written as function of time:

$$\gamma(t) = \frac{R_{head}(t)}{2}\left[\Delta p_{AB}(t) - \Delta p_{f,AB}\right] \tag{27}$$

with $\Delta p_{f,AB}$ the constant resistance in the flow path, Δp_{AB} experimentally measured and R_{head} the radius of the droplet measured in the horizontally direction through time.

The volume of the droplets is determined by tracking the size with a high-speed camera. This allows identifying 3 stages in the droplet formation process, as shown in Fig. 10. During the first step (from I to II), the dispersed phase confined in the capillary is flowing to the increasingly narrower tip, which leads to an increase of the Laplace pressure. Then, it is first followed by a rapid growth of the droplet (from II to III), which very quickly turns into a stable volumetric growth stage (from III to IV). Interfacial tension is deduced from the stable growth stage and the flow resistance $\Delta p_{f,AB}$ is calculated by using a classic droplet scaling law (see Eq. 30), at the moment of droplet release.

This article shows that droplet formation in this device is not affected by Marangoni effects evaluated as follows from the Marangoni number Ma:

$$Ma = \frac{E}{Ca} \approx \frac{\gamma_0 - \gamma}{\eta_C U_c} \tag{28}$$

Table 3
Microfluidic devices comparison for the determination of interfacial properties.

Measurement method	Interface	Equation $\gamma(t)$	Measurement time scale	Sources of uncertainties	Reference
Laplace pressure	A/W and O/W	$\gamma(t) = \frac{1}{2}\Delta P(t).R(t)$	$\tau_m > 1$ s	Determination of the radius through imaging, pressure drop measurement	Alvarez et al. [87]
Laplace pressure	A/W and O/W	$\gamma(t) = \frac{h.P_d(t)}{2cos(\theta)}$	$\tau_m > 1$ ms	Pressure determination, contact angle	Deng et al. [116]
Laplace pressure	O/W	$\gamma(t) = \frac{R_{head}(t)}{2}\left[\Delta p_{AB}(t) - \Delta p_{f,AB}\right]$	$\tau_m > 10$ ms	Pressure determination	Liang et al. [119]
Droplet volume	O/W	$\gamma \propto \frac{Q_d}{\sqrt{Ca}}$	0.4 ms $< \tau_m <$ 9.4 ms	Imaging	Muijlwijk et al. [122]
Droplet diameter	O/W	–	$\tau_m > 5$ *ms*	Droplet diameter measurements	Wang et al. [126]
Droplet diameter	O/W	–	2.8 *ms* $< \tau_m <$ 64.5 *ms*	Droplet diameter measurements	Kalli et al. [127]
Dripping/jetting transition	O/W	Rayleigh-Plateau instability	$\tau_m > 85$ *ms*	Flow rates controller	Moiré et al. [118]

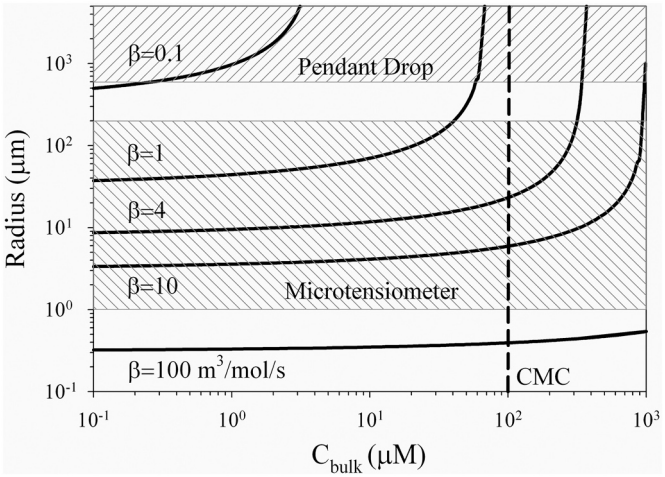

Fig. 8. Operating diagram showing bubble radius and bulk surfactant concentration. The solid lines correspond to the points where the kinetic and diffusion time scales are equal for a given adsorption constant. Here, β is the adsorption constant referred as k_a in our text ($\beta = k_a$). Far to the left of the solid line, it defines diffusion-limited dynamics and far to the right of the line, it defines kinetic-limited dynamics. The two shaded regions correspond to the experimental operating regimes for the pendant drop/bubble and the microtensiometer apparatus. Reprinted with permission from Alvarez et al. [87]. Copyright 2010, American Chemical Society.

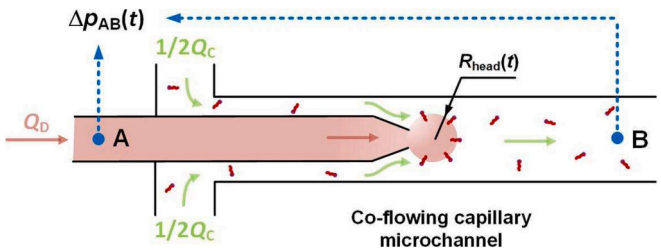

Fig. 9. Schematic diagram of the differential pressure measurement. Reprinted from Liang et al. [119]. Copyright 2022 with permission from Elsevier.

with E the elasticity number estimated by $(\gamma_0 - \gamma)/\gamma$, Ca the capillary number, η_c and U_c the dynamic viscosity and mean velocity of the continuous phase, respectively. Dynamic interfacial tension was fitted using the Frumkin isotherm, from which adsorption rates were extracted and discussed [119]. This article stresses the complexity of droplet formation and has successfully identified the crucial steps to estimate the surfactant adsorption time.

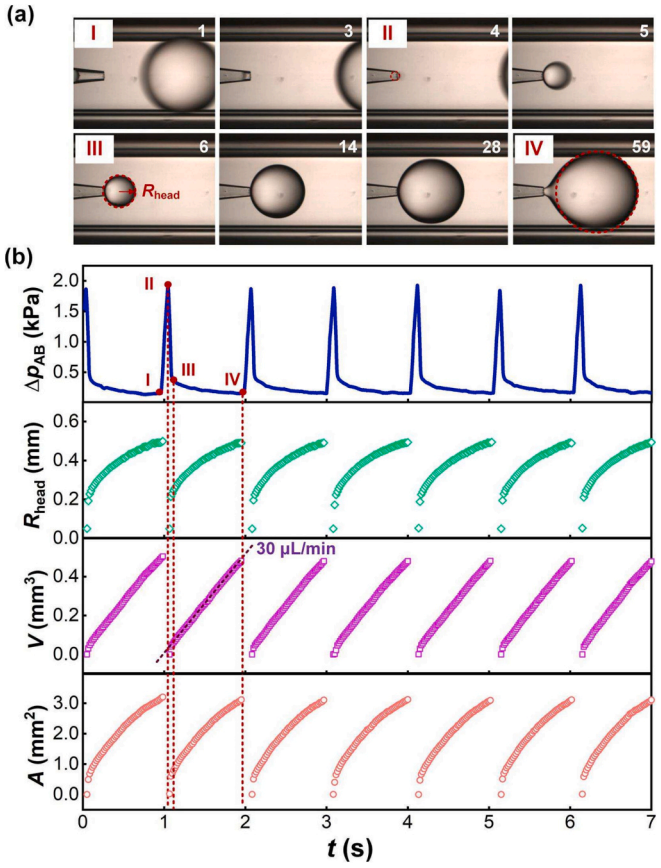

Fig. 10. Droplet formation process in the microfluidic device. (a) Images taken during droplet formation. (b) Variations of Δp_{AB} (including a link to the images in (a) through roman numbers), R_{head}, volume V and interfacial area A during repeated droplet formation processes. $Q_d = 30\ \mu L/min$ and $Q_c = 900\ \mu L/min$, droplet generation frequency was 1.0 *Hz*. Reprinted from Liang et al. [119]. Copyright 2022 with permission from Elsevier.

The Laplace pressure method has also been used in a completely different apparatus, the Edge-based Droplet GEneration (EDGE) device to measure dynamic interfacial tension [116]. These devices, also called STEP, are initially used to generate monodisperse emulsions [120] but interfacial properties can also be determined with the EDGE apparatus [116,121]. In 2022, Deng et al. [116] have used the EDGE apparatus as a tensiometer to study dynamic interfacial tension of SDS solutions at the air/water and oil/water interface. The apparatus (Fig. 11) is made of a plateau with several pores, across which the dispersed phase forms

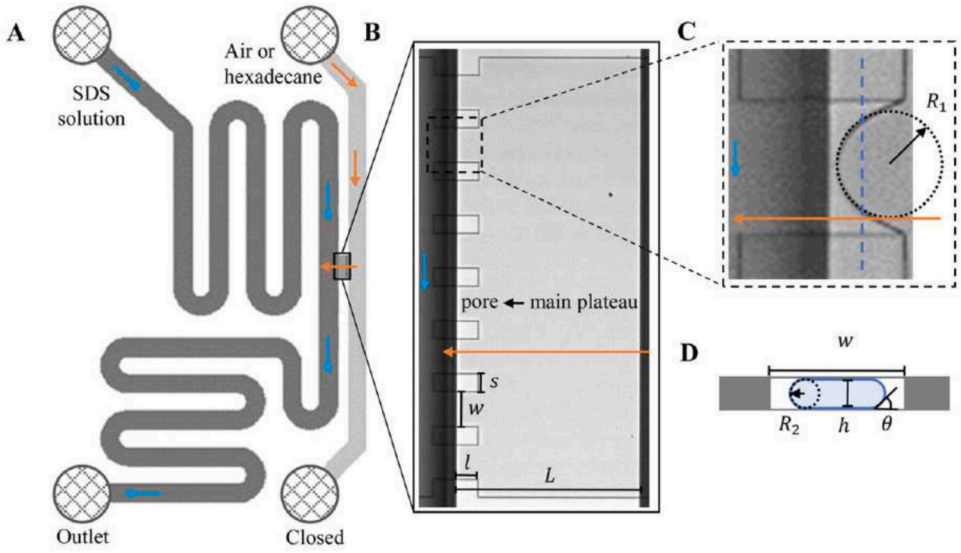

Fig. 11. A: schematic illustration of the partitioned-EDGE device. B: microscopy image of the main plateau and pores. C and D illustrate the two radii of curvature across the meniscus with C the top-view (microscopy) and D the head-on view of the pore (schematic, for the location indicated by a dashed blue line shown in C, not drawn to scale). In A–C, it is noted that the partition features extend into the continuous phase channel, yet at that side of the main plateau they do not interfere with droplet or bubble formation as their height (h) is much smaller than that of the deep channel; the flow of the continuous and dispersed phases is indicated by blue and orange arrows, respectively. From Deng et al. [116]. (For interpretation of the references to colour in this figure legend, the reader is referred to the web version of this article.)

droplets or bubbles. These are then flushed by the continuous phase. The initiation of formation at each pore is governed by the equilibrium between the Laplace pressure within the pore and the externally applied pressure. The force balance is reached when enough surfactant molecules have adsorbed at the interface, decreasing the interfacial tension and therefore the Laplace pressure. Deng et al. [116] have studied the droplet formation in EDGE devices detail. They suggest a three-step process with as many characteristic times: adsorption time, filling time (during which the pore is filled by the dispersed phase) and the necking time corresponding to the droplet formation. The time of droplet formation and the return to the initial stage is about 10 μs, which is much smaller than the adsorption time. Therefore, the mass-transfer rate of the surfactant can be very well approximated by the frequency of the droplet formation [116].

While the determination of the interfacial tension is relatively straightforward by applying a specific pressure and monitoring droplets or bubbles over a set time period, the wettability in the pore is a crucial parameter. Indeed, according to Laplace pressure, and the geometry of the partitioned EDGE device [116] the interfacial tension is calculated as follows:

$$\gamma(t) = \frac{h.P_d(t)}{2cos(\theta)} \tag{29}$$

and the contact angle θ has to be correctly evaluated. The authors have validated the method by measurement of the dynamic interfacial tension of a well-studied ionic surfactant SDS at the air/water and hexadecane/water interfaces. Their results were compared with a the pendant drop tensiometer and a Y-junction as shown in the Fig. 12.

As we can see, both microfluidic devices reach shorter time scales, comparable with droplet and bubble formation in industrial processes (sub-millisecond), while conventional pendant drop tensiometer is more suited for equilibrium study. From the discrepancies of the curves between each method, Deng et al. [116] have concluded that different mechanisms are observed. While the pendant drop clearly displays a diffusion-limited mass-transfer, the Y-junction [122] and the EDGE, thanks to high curvatures and convective flows, are able to catch mixed-diffusion or kinetics limited mechanisms.

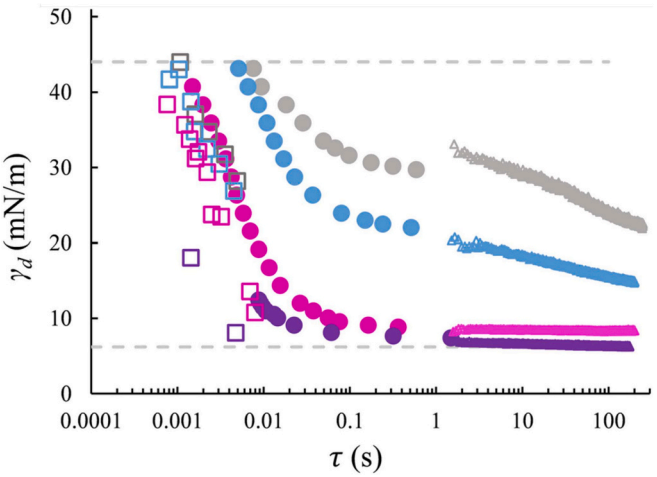

Fig. 12. Dynamic interfacial tension versus time obtained with Y-junction (squares), EDGE tensiometer (circles), and pendant drop technique (triangles). The comparison is illustrated with four SDS concentrations: 0.05% wt (grey), 0.1% wt (blue), 0.3% wt (pink), and 1% wt (purple). The data sets for Y-junction and pendant drop are adapted from Muijlwijk et al. (2016) [122]. Comparison from Deng et al. (2022) [116]. (For interpretation of the references to colour in this figure legend, the reader is referred to the web version of this article.)

4.1.2. *Dynamic interfacial tension measurements based on droplet shape*

Since the beginning of microfluidics, different geometries have been developed to generate droplets, such as the Y-junction [122] and T-junction [33,123] in which droplet formation has been extensively studied by Glawdel et al. in two papers [124,125]. The size of the droplet primarily results from the equilibrium between the shear force and interfacial tension, that is usually quantified by the Capillary number *Ca*, expressed as follows:

$$Ca = \frac{\eta_c Q_c}{A\gamma} = \frac{\eta_c v_c}{\gamma} \tag{30}$$

with η_c the dynamic viscosity of the continuous phase in *Pa.s*, Q_c the flow rate of the continuous phase in m^3/s, A the section area of the microfluidic channel and γ the interfacial tension at the moment the droplet/bubble detaches. In 2016, Muijlwijk et al. [122] have modeled the two-steps process of droplet formation in a Y-junction and managed to scale the volume of the droplet to the interfacial tension, as a function of $1/\sqrt{Ca}$ and flow rate of the dispersed phase. They have validated their model with solutions of ionic surfactant SDS at the water/hexadecane interface. With this method, they were able to measure dynamic interfacial tension for droplet formation of 0.4 to 9.4 *ms*.

Another method was used by Wang et al. [126] in three Y-junction devices, where the droplet diameter is measured and scaled with flow rates of both phases and capillary number. For all three apparatus, of which the geometry is very similar, the following relation was found to be in agreement with their experiments:

$$\frac{d_{av}}{d_s} = 1.218\left(\frac{Q_D}{Q_C}\right)^{0.125} Ca^{-0.184} \tag{31}$$

with d_{av} the average droplet diameter and d_s a characteristic length scale of the device (usually the smallest structural parameter of the microfluidic device). Interfacial tension is then deduced from the capillary number definition and characteristic parameters of the systems. Experiments were carried out for classical surfactants: SDS, DTAB, Triton X-100 and Tween 20.

Droplet size measurements have also been used to study dynamic interfacial properties by Kalli et al. [127] who studied SDS, DTAB and Triton X-100 surfactants at the water/silicone oil interface with a cross-junction in a glass microchannel. As done by others [123,126], the droplet size has been scaled with flow rates of both continuous and dispersed phase and with the capillary number. The experimental data were then fitted with the following expression:

$$\frac{d_{av}}{d_s} = 0.642\left(\frac{Q_D}{Q_C}\right)^{0.188} Ca^{-0.161} \tag{32}$$

with d_{av} the average droplet diameter and d_s the characteristic length of the device, such as the channel width (195 μm in this device). The coefficients differ slightly from the ones found by Wang et al. [126], who used Y-junction microfluidic devices instead of cross-junction. The scaling needs to be studied for each specific geometry. In both papers, the authors [126,127] have managed to measure dynamic interfacial tension at short times around 5 *ms* (and even down to 3 *ms* for [127]), for diluted surfactant solutions.

In these devices, adsorption time is not directly deduced from the experiment, such as done in the EDGE device [116]. Wang et al. [126] and Kalli et al. [127] estimate the mass-transport time using characteristic numbers based on the study of Alvarez et al. [106] and the theoretical time of diffusion: $\tau_m = \frac{min(h_p,h_c)^2}{D}$, where $h_p = \frac{\Gamma_{eq}}{c_{bulk}}$ and $h_c = \left(\frac{2\pi}{3Pe}\right)^{1/2} R$ with R the droplet radius and Pe the Peclet number. This scaling approach has been well described by Alvarez et al. [106] and is further detailed in subsection 4.2.

4.1.3. Other microfluidic devices for dynamic interfacial tension measurements

While the previous apparatus described rely mostly on droplet formation and droplet size or shape, Moiré et al. [118] have built a microfluidic tensiometer based on the transition between two hydrodynamic regimes. According to the flow rates, either droplets or jets can be observed in the apparatus. Based on a previous work [117], it has been shown that the transition between the two regimes relies on the Rayleigh-Plateau instability. The determination of the dynamic interfacial tension requires the building of a flow diagram, where continuous and dispersed flow rates are displayed according to the hydrodynamic regime encountered. The interfacial tension is found by a hydrodynamic model of the Rayleigh-plateau instability in the cylindrical geometry given by [117]. With this method, no droplet size or shape determination is required.

The mass transfer time is a bit more difficult to determine than in other microfluidic tensiometers. For the characteristic time for surfactant mass transfer, the authors used the same approach as Wang et al. [126]. They compared τ_m (see subsubsection 4.1.2), with the microfluidic time τ_μ calculated as: $\tau_\mu = \frac{R}{U_i}$ with U_i the mean velocity of the internal phase. The microfluidic time is an estimation of the surfactant mass transport time, but it is difficult to conclude underlying mechanisms from it. Note that for solutions at concentration above the *cmc*, the diffusion coefficient can be replaced by an apparent coefficient D_{eff} [124] (see Eq. 19). Nevertheless, Moiré et al. [118] have been able to study interfacial tension for Triton X-100 and CTAB systems at the water/oil interface. Furthermore, ultralow interfacial tensions could be measured down to 2×10^{-3} mN/m and performed at a time $\tau_m > 85$ *ms*.

Table 3 summarizes the different microfluidic apparatus reviewed in this part with their measurement time scale, method and source of uncertainties.

4.2. Example of studies measuring the kinetics parameters using microfluidic devices

Despite their performance, to date there have been very few experiments using microfluidics to measure the adsorption kinetic constants of the surfactants. In a microfluidic device, convection plays an important role and must be taken into account. Let us first underline that the orientation of the velocity with respect to the droplet interface is an important parameter. If the velocity is colinear with the droplet normal, convection not only modifies the diffusion length, it also brings material directly onto the droplet, which reinforces the fact that the limiting stage is adsorption. None of the tensiometers presented above are in this configuration. Generally in microfluidics, the velocity is parallel to the interface and modifies the depletion layer as studied by Alvarez [106]. The analysis presented by Riechers should be repeated and convection times taken into account [15].

Alvarez's apparatus is composed of a capillary inserted into a chamber made of PDMS. The authors have measured dynamic surface tension as a function of the Peclet number which compares advection forces over diffusion and is defined as follows:

$$Pe = \frac{vL}{D} \tag{33}$$

with v the characteristic flow velocity, L a characteristic length scale and D the diffusion coefficient. In their apparatus, the idea is to use the convection flow near the spherical interface to reduce the diffusion boundary layer thickness and therefore decrease the time-scale for diffusion. They have built a mathematical model for mass transport considering convection flow, and expressed the effective boundary layer thickness h, for a rigid sphere and a mobile spherical interface. For a rigid sphere, h_{cR} scales as:

$$h_{cR} \approx \left(\frac{4}{3Pe}\right)^{1/3} R \tag{34}$$

and considering a mobile interface with no shear stress:

$$h_{cM} \approx \left(\frac{2\pi}{3Pe}\right)^{1/2} R \tag{35}$$

with R the radius of the bubble/droplet that usually varies from $10\mu m$ to $200\mu m$ [106]. Therefore, the diffusion times scale as $\tau_{DR} \propto Pe^{-2/3}$ for a rigid interface and $\tau_{DM} \propto Pe^{-1}$, for a mobile one. These expressions are valid for $Re < 1$ [106]. The authors have done simulations for $C_{12}E_8$ and

$C_{14}E_8$ solutions at different concentrations and compared with experimental results. Fig. 13 shows the experimental time scale required to reach a certain value of IFT for $C_{14}E_8$ solutions. The same analysis was conducted for $C_{12}E_8$ solutions. Fig. 13 shows that for the whole *Pe* number range, the numerical simulation for a rigid interface better fits the experimental points than for a mobile interface.

In their study Alvarez et al. [106] show that there is no observable transition between diffusion-limited and mixed or kinetically-limited dynamics at the air/water interface for $C_{12}E_8$ and $C_{14}E_8$ when $Pe < 10^5$. Whatever the situation, the evolution of surface tension is governed by diffusion. Using a kinetically limited model, they establish lower limits for the adsorption coefficient of both surfactants. The kinetic adsorption coefficients for $C_{12}E_8$ and $C_{14}E_8$ exceed 17 and 23 $m^3/(mol.s)$ respectively. These values significantly exceed those documented in the literature, implying that the previously reported figures underestimated the complexities involved in extracting kinetic data from diffusion-controlled processes. Therefore, the utilisation of convective flow could be beneficial in accurately assessing these parameters by reaching the kinetic regime.

This microfluidic study does not provide a study of the adsorption parameters, which are very rapid, but it does give a way of achieving these measurements.

Using a slower system, Brosseau et al. [66] were able to measure these kinetics. They designed a microfluidic tensiometer in which adsorption at the interface is the limiting step for a block copolymer perfluoro surfactant at the oil/water interface (perfluoro molecules in the oil phase). The DIFT measurements are based on droplet deformation and the authors are able to measure it at the millisecond scale. First, crucial interfacial parameters such as maximum surface coverage Γ_∞ and diffusion coefficient D are determined by classical pendant drop tensiometry and by fitting the Ward and Tordai [35] diffusion model. Then, the adsorption kinetics is determined with a correlation scaling with the capillary number $Ca = \eta U/\gamma$ with η the viscosity of the continuous phase and U the characteristic velocity (i.e drop velocity here). *Ca* is scaled with the maximum deformation of the droplet δ_{max} and a characteristic length scale due to the geometry. δ_{max} is determined by camera analysis further explained in the methods part of the article [66]. An empirical scaling of γ as a function of droplet deformation parameter is used to deduce interfacial tension.

In the microfluidic device, the interfacial tension has successfully been fitted with an exponential relaxation, sign of a kinetics-limited system. In fact, for a diffusion-controlled mechanism, interfacial tension scales as $t^{1/2}$ at short time and $t^{3/2}$ at longer time [39]. Equilibrium values were also obtained with the same set-up and the results were in agreement with pendant drop experiments. Fig. 14 shows the maximum deformation and the surface tension deduced from it at the time scale from the millisecond to more than two seconds. Experimental data from Fig. 11 b) were fitted with the following scaling: $\gamma - \gamma_{eq} \propto exp(-t/\tau)$ where:

$$\tau = \frac{1}{k_d}\frac{1}{1+K_L c} \tag{36}$$

with K_L the Langmuir's constant defined in section 2. As we can see in Fig. 14, the fit is in good agreement with experimental data and they have been able to extract interfacial parameters for a kinetic-limited system. In their system, the cutoff length R_{DK} [86] or R^* [15] dissociating adsorption and diffusion processes is around 10 μm. The *Pe* number is of the order of 10^5 so convection is strong in the microfluidic device, leading to an adsorption limited mass transfer even for droplets of 100 μm. In this paper, the authors have been able to study the adsorption step of one type of surfactant (PEG-PFPE polymer) at the oil/water interface. Diffusion does not play a critical role in this process due to convective effects in microfluidic channels. Experiments were also carried with the pendant drop where mass-transfer is clearly diffusion limited according to the fits and scales. The length cutoff R^*, given by a Langmuir process, is particularly suited for the determination of the controlling step in droplets. This paper essentially presents theoretical and computational assessments of the different effects in surfactant mass-transfer.

We have shown that with microfluidic devices, interfacial tension measurements can be performed in conditions where diffusion is not the only driving mechanism for surfactant mass transport at the interface. Therefore, these new microfluidic tools pave the way of a more accurate study of surfactant mass transport at different scales. Compared to classical tensiometers, for some microfluidic devices, it can be challenging to directly determine the mass transport time, especially when it is of the same order of magnitude as the droplet or bubble formation time. It is noteworthy that technical challenges still need to be tackled to implement these devices for high-throughput experiments. Finally, the different hydrodynamic conditions we found in microfluidics could also benefit from numerical simulations to predict surfactant mass transport with consideration of fluid flows [128].

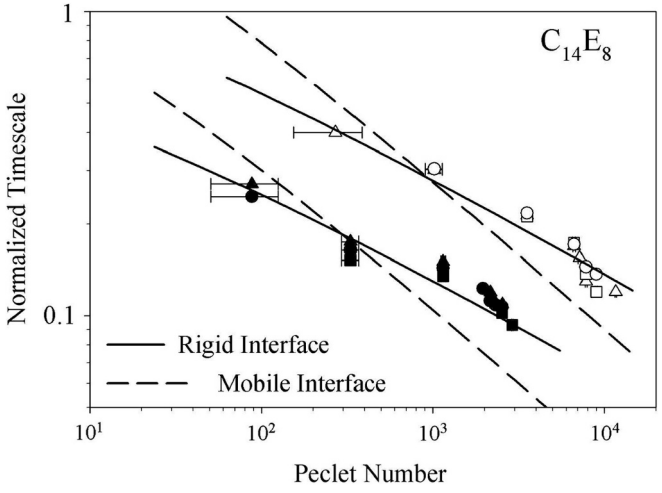

Fig. 13. Experimental timescale required to reach $\gamma_t = 60mN/m$ for $C_{14}E_8$ for three concentrations (● 0.0025 mol/m^3; ■ 0.003 mol/m^3 and ▼ 0.004 mol/m^3) and two radii $R = 60\mu m$ filled symbols, $R = 185\mu m$ open symbols as a function of *Pe* number compared with predicted scaling for diffusion-limited system for a rigid interface and a mobile interface. Reprinted from Alvarez et al. [106]. Copyright 2012 with permission from Elsevier.

5. Conclusion and prospects

In this review we pointed out the importance of knowing the value of the surface tension and, more precisely, its value as a function of time. This has led us to propose two strategies for working on the dimensioning of a process involving interface creation. The first strategy consists of mimicking interface creation using the time range characteristic of the process. This strategy is not rigorous, as it is difficult to be certain that adsorption and diffusion conditions will be identical in the process and in the experiment dedicated to the measurement. The second strategy is to directly measure the parameters involved in each of these two processes. Our review shows that diffusion coefficient measurements and surface tension characterisation can be performed using dynamic tension measurements on conventional tensiometers with large droplets. When high kinetic barriers are assumed, short times and low concentrations are preferred. Measuring kinetic coefficients is more complex, because even if adsorption dynamics interfere with mass transport mechanisms, they are almost never preponderant when studies focus on large droplets. Studies show that so-called mixed models can be used to account for the evolution of dynamic interfacial tension. However, these techniques are imprecise to say the least. Microfluidics and the new tensiometers seem to provide an answer to these questions, at least in the context of slow systems, as shown by

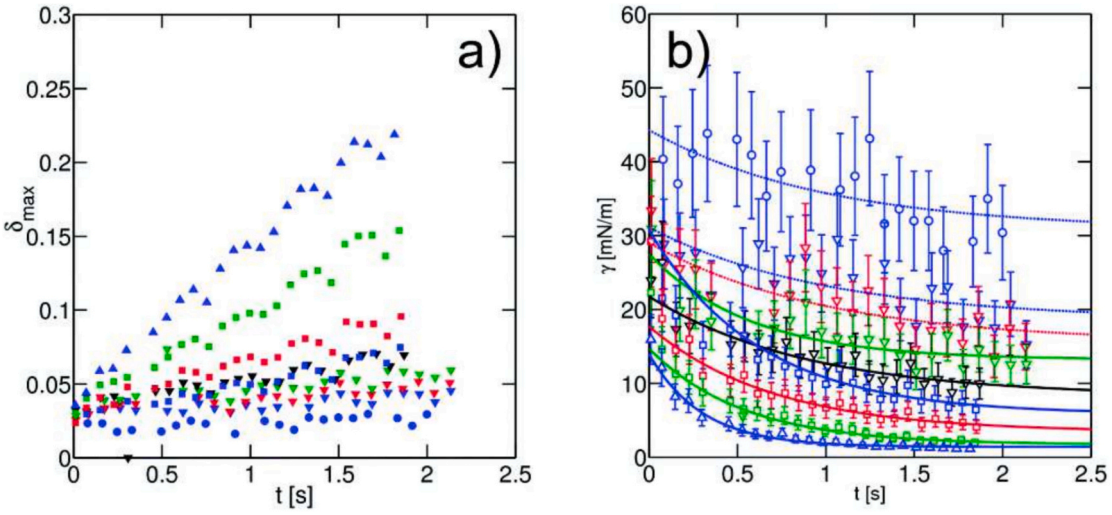

Fig. 14. (a) Maximum deformation of the droplet as a function of the time as recorded on-chip. Here the measured points correspond to a subset where one chamber out of five is analysed. The concentrations of surfactant used are: $C = 1.3 \times 10^{-3} mol/m^3$ (●); $C = 1.3 \times 10^{-2} mol/m^3$ (▼); $C = 2.6 \times 10^{-2} mol/m^3$ (▼); $C = 5.2 \times 10^{-2} mol/m^3$ (▼); $C = 10.4 \times 10^{-2} mol/m^3$ (▼); $C = 1.3 \times 10^{-1} mol/m^3$ (■); $C = 2.6 \times 10^{-1} mol/m^3$ (■); $C = 5.2 \times 10^{-1} mol/m^3$ (■); $C = 1.3 \times mol/m^3$ (▲). (b) Surface tension derived from the maximum droplet deformation with the empirical scaling. The open symbols correspond to the concentration in (a). The solid lines are the best fits found for each concentration, using an exponential fitting of the late kinetics, based on exponential scaling. For the dotted line the fit has been done with values of the Langmuir characteristic time τ (Eq. 36) fixed to one in order to extract the equilibrium surface tension. From Brosseau et al. [66].

Brosseau [66]. Such experiments need to be carried out on a large number of surfactants to find the kinetic constants. Using a flow velocity along the normal to the droplet interface may be a solution. It is necessary to think about such geometries. Brosseau's study enables us to measure the kinetic constant. However, it raises some fundamental thermodynamic questions. Is it reasonable to describe the relationship between coverage rate and surface tension, assuming that this relationship is the same as when the adsorption layer and the sublayer are in equilibrium? This is what is done in mixed models. Brosseau does not use this approximation, as he empirically assumes that surface tension decreases exponentially with the same material time as the coverage rate. Both theoretical and experimental studies are needed to clarify this point.

In this review, we have highlighted the importance of knowing each mechanism for surfactant mass transport at interfaces for a wide range of time scales and processes. The experimental methods coupled with theoretical models reviewed in this article show it is possible to study more accurately interfacial phenomena in conditions similar to the ones encountered in different processes.

CRediT authorship contribution statement

Camille Brigodiot: Writing – review & editing, Writing – original draft, Validation, Investigation, Conceptualization. **Marie Marsiglia:** Writing – review & editing, Validation, Supervision, Conceptualization. **Christine Dalmazzone:** Writing – review & editing, Validation, Supervision, Conceptualization. **Karin Schroën:** Writing – review & editing, Validation, Supervision, Conceptualization. **Annie Colin:** Writing – review & editing, Validation, Supervision, Conceptualization.

Declaration of competing interest

The authors declare that they have no known competing financial interests or personal relationships that could have appeared to influence the work reported in this paper.

Data availability

No data was used for the research described in the article.

Acknowledgements

This investigation is supported by IFP Energies nouvelles doctorate fundings.

References

[1] De Gennes P-G, Brochard-Wyart F, Quéré D. Gouttes, bulles, perles et ondes. Belin Paris. 2002.
[2] Guyon É, Hulin J-P, Petit L. Ce que disent les fluides: la science des écoulements en images. Broché; 2005.
[3] Bouasse H. Capillarite: phenomenes superficiels. Delagrave 1924.
[4] Pallas N, Pethica B. The surface tension of water. Colloids Surf 1983;6(3):221–7.
[5] Facchini MC, Mircea M, Fuzzi S, Charlson RJ. Cloud albedo enhancement by surface-active organic solutes in growing droplets. Nature 1999;401(6750):257–9.
[6] Swarup S, Schoff CK. A survey of surfactants in coatings technology. Prog Org Coat 1993;23(1):1–22.
[7] Wang T, Chang D, Huang D, Liu Z, Wu Y, Liu H, et al. Application of surfactants in papermaking industry and future development trend of green surfactants. Appl Microbiol Biotechnol 2021:1–16.
[8] Jun H-Y, Kim S-J, Choi C-H. Ink formulation and printing parameters for inkjet printing of two dimensional materials: a mini review. Nanomaterials 2021;11(12):3441.
[9] Ellis MB, Tuck C, Miller P. How surface tension of surfactant solutions influences the characteristics of sprays produced by hydraulic nozzles used for pesticide application. Colloids Surf A Physicochem Eng Asp 2001;180(3):267–76.
[10] A. A. Maan, K. Schroën, and R. Boom, "Spontaneous droplet formation techniques for monodisperse emulsions preparation–perspectives for food applications," J Food Eng, vol. 107, no. 3–4, pp. 334–346, 2011.
[11] Nazir A, Schroën K, Boom R. The effect of pore geometry on premix membrane emulsification using nickel sieves having uniform pores. Chem Eng Sci 2013;93:173–80.
[12] Malysa K, Krasowska M, Krzan M. Influence of surface active substances on bubble motion and collision with various interfaces. Adv Colloid Interface Sci 2005;114:205–25.
[13] Schultz S, Wagner G, Urban K, Ulrich J. High-pressure homogenization as a process for emulsion formation. Chem Eng Technol Indust Chem Plant Equip Process Eng Biotechnol 2004;27(4):361–8.
[14] Schroën K, de Ruiter J, Berton-Carabin C. The importance of interfacial tension in emulsification: connecting scaling relations used in large scale preparation with microfluidic measurement methods. ChemEngineering 2020;4(4):63.
[15] Riechers B, Maes F, Akoury E, Semin B, Gruner P, Baret J-C. Surfactant adsorption kinetics in microfluidics. Proc Natl Acad Sci U S A 2016;113(41):11465–70.
[16] Bhardwaj A, Hartland S. Dynamics of emulsification and demulsification of water in crude oil emulsions. Indust Eng Chem Res 1994;33(5):1271–9.
[17] Shehzad F, Hussein IA, Kamal MS, Ahmad W, Sultan AS, Nasser MS. Polymeric surfactants and emerging alternatives used in the demulsification of produced water: a review. Polym Rev 2018;58(1):63–101.

[18] Yao L, Selmi A, Esmaeili H. A review study on new aspects of biodemulsifiers: production, features and their application in wastewater treatment. Chemosphere 2021;284:131364.
[19] Taylor KC, Schramm LL. Measurement of short-term low dynamic interfacial tensions: application to surfactant enhanced alkaline flooding in enhanced oil recovery. Colloids Surf 1990;47:245–53.
[20] Al-Sabagh AM, Kandile NG, Noor El-Din MR. Functions of demulsifiers in the petroleum industry. Sep Sci Technol 2011;46(7):1144–63.
[21] Rajasimman M, Sangeetha R, Karthik P. Statistical optimization of process parameters for the extraction of chromium (vi) from pharmaceutical wastewater by emulsion liquid membrane. Chem Eng J 2009;150(2–3):275–9.
[22] Muthusaravanan S, Priyadharshini SV, Sivarajasekar N, Subashini R, Sivamani S, Dharaskar S, et al. Optimization and extraction of pharmaceutical micro-pollutant-norfloxacin using green emulsion liquid membranes. Desalin Water Treat 2019;156:238–44.
[23] Krawczyk MA, Wasan DT, Shetty C. Chemical demulsification of petroleum emulsions using oil-soluble demulsifiers. Indust Eng Chem Res 1991;30(2):367–75.
[24] Hussein MA, Mohammed AA, Atiya MA. Application of emulsion and Pickering emulsion liquid membrane technique for wastewater treatment: an overview. Environ Sci Pollut Res 2019;26:36184–204.
[25] Gricius Z, Øye G. Recent advances in the design and use of Pickering emulsions for wastewater treatment applications. Soft Matter 2023;(19):818–40.
[26] Van der Graaf S, Schroën C, Van der Sman R, Boom R. Influence of dynamic interfacial tension on droplet formation during membrane emulsification. J Colloid Interface Sci 2004;277(2):456–63.
[27] Liang T-B, Slater M. Liquid—liquid extraction drop formation: mass transfer and the influence of surfactant. Chem Eng Sci 1990;45(1):97–105.
[28] Kralj JG, Schmidt MA, Jensen KF. Surfactant-enhanced liquid–liquid extraction in microfluidic channels with inline electric-field enhanced coalescence. Lab Chip 2005;5(5):531–5.
[29] Mazzola PG, Lopes AM, Hasmann FA, Jozala AF, Penna TC, Magalhaes PO, et al. Liquid–liquid extraction of biomolecules: an overview and update of the main techniques. J Chem Technol Biotechnol Int Res Process Environ Clean Technol 2008;83(2):143–57.
[30] Miller R, Joos P, Fainerman VB. Dynamic surface and interfacial tensions of surfactant and polymer solutions. Adv Colloid Interface Sci 1994;49:249–302.
[31] Aronson MP. The role of free surfactant in destabilizing oil-in-water emulsions. Langmuir 1989;5(2):494–501.
[32] Walstra P. Principles of emulsion formation. Chem Eng Sci 1993;48(2):333–49.
[33] Wang K, Lu Y, Xu J, Luo G. Determination of dynamic interfacial tension and its effect on droplet formation in the t-shaped microdispersion process. Langmuir 2009;25(4):2153–8.
[34] Walstra P. Principles of foam formation and stability. In: Foams: Physics, chemistry and structure. Springer; 1989. p. 1–15.
[35] Ward AFH, Tordai L. Existence of time-dependence for interfacial tension of solutions. Nature 1944;154(3900):146–7.
[36] Chang C-H, Franses EI. Adsorption dynamics of surfactants at the air/water interface: a critical review of mathematical models, data, and mechanisms. Colloids Surf A Physicochem Eng Asp 1995;100:1–45.
[37] Ferri JK, Gorevski N, Kotsmar C, Leser ME, Miller R. Desorption kinetics of surfactants at fluid interfaces by novel coaxial capillary pendant drop experiments. Colloids Surf A Physicochem Eng Asp 2008;319(1–3):13–20.
[38] Svitova T, Wetherbee M, Radke C. Dynamics of surfactant sorption at the air/water interface: continuous-flow tensiometry. J Colloid Interface Sci 2003;261(1):170–9.
[39] Ward AFH, Tordai L. Time–dependence of boundary tensions of solutions i. the role of diffusion in time–effects. J Chem Phys 1946;14(7):453–61.
[40] Bellocq A, Biais J, Bothorel P, Clin B, Fourche G, Lalanne P, et al. Microemulsions. Adv Colloid Interface Sci 1984;20(3–4):167–272.
[41] H. Watarai, "Microemulsions in separation sciences," J Chromatogr A, vol. 780, no. 1–2, pp. 93–102, 1997.
[42] Ravera F, Ferrari M, Liggieri L. Adsorption and partitioning of surfactants in liquid-liquid systems. Adv Colloid Interface Sci 2000;88(1–2):129–77.
[43] Owens DK. The dynamic surface tension of sodium dodecyl sulfate solutions. J Colloid Interface Sci 1969;29(3):496–501.
[44] Mucic N, Kovalchuk NM, Pradines V, Javadi A, Aksenenko EV, Krägel J, et al. Dynamic properties of cntab adsorption layers at the water/oil interface. Colloids Surf A Physicochem Eng Asp 2014;441:825–30.
[45] Miller R, Aksenenko EV, Fainerman VB. Dynamic interfacial tension of surfactant solutions. Adv Colloid Interface Sci 2017;247:115–29.
[46] Kroll P, Benke J, Enders S, Brandenbusch C, Sadowski G. Influence of temperature and concentration on the self-assembly of nonionic ciej surfactants: a light scattering study. ACS omega 2022;7(8):7057–65.
[47] Gilányi T, Varga I, Gilányi M, Mészáros R. Adsorption of poly(ethylene oxide) at the air/water interface: a dynamic and static surface tension study. J Colloid Interface Sci 2006;301(2):428–35.
[48] Langmuir I. The constitution and fundamental properties of solids and liquids. Part i. solids. J Am Chem Soc 1916;38(11):2221–95.
[49] Lee Y-C, Stebe KJ, Liu H-S, Lin S-Y. Adsorption and desorption kinetics of cme8 on impulsively expanded or compressed air–water interfaces. Colloids Surf A Physicochem Eng Asp 2003;220(1–3):139–50.
[50] Prosser AJ, Franses EI. Adsorption and surface tension of ionic surfactants at the air–water interface: review and evaluation of equilibrium models. Colloids Surf A Physicochem Eng Asp 2001;178(1–3):1–40.
[51] Eastoe J, Dalton J. Dynamic surface tension and adsorption mechanisms of surfactants at the air–water interface. Adv Colloid Interface Sci 2000;85(2–3):103–44.
[52] Lin SY, McKeigue K, Maldarelli C. Diffusion-limited interpretation of the induction period in the relaxation in surface tension due to the adsorption of straight chain, small polar group surfactants: theory and experiment. Langmuir 1991;7(6):1055–66.
[53] Wang J, Guo X. Adsorption isotherm models: classification, physical meaning, application and solving method. Chemosphere 2020;258:127279.
[54] Liggieri L, Ravera F, Ferrari M, Passerone A, Miller R. Adsorption kinetics of alkylphosphine oxides at water/hexane interface: 2. Theory of the adsorption with transport across the interface in finite systems. J Colloid Interface Sci 1997;186(1):46–52.
[55] Chang H-C, Hsu C-T, Lin S-Y. Adsorption kinetics of c10e8 at the air-water interface. Langmuir 1998;14(9):2476–84.
[56] Manglik RM, Wasekar VM, Zhang J. Dynamic and equilibrium surface tension of aqueous surfactant and polymeric solutions. Exp Thermal Fluid Sci 2001;25(1–2):55–64.
[57] Lin S-Y, Lee Y-C, Yang M-W, Liu H-S. Surface equation of state of nonionic c m e n surfactants. Langmuir 2003;19(8):3164–71.
[58] Lin S-Y, Lee Y-C, Shao M-J, Hsu C-T. A study on surfactant adsorption kinetics: the role of the data of equation of state γ (γ) for c14e8. J Colloid Interface Sci 2001;244(2):372–6.
[59] Lee Y-C, Lin S-Y, Liu H-S. Role of equation of state on studying surfactant adsorption kinetics. Langmuir 2001;17(20):6196–202.
[60] Milner S. Iv. On surface concentration, and the formation of liquid films. London Edinburgh Dublin Philos Mag J Sci 1907;13(73):96–110.
[61] Lin S-Y, McKeigue K, Maldarelli C. Diffusion-controlled surfactant adsorption studied by pendant drop digitization. AIChE Journal 1990;36(12):1785–95.
[62] Reichert MD, Alvarez NJ, Brooks CF, Grillet AM, Mondy LA, Anna SL, et al. The importance of experimental design on measurement of dynamic interfacial tension and interfacial rheology in diffusion-limited surfactant systems. Colloids Surf A Physicochem Eng Asp 2015;467:135–42.
[63] Alvarez NJ, Walker LM, Anna SL. Diffusion-limited adsorption to a spherical geometry: the impact of curvature and competitive time scales. Physical Review E 2010;82(1):011604.
[64] Baret J. Theoretical model for an interface allowing a kinetic study of adsorption. J Colloid Interface Sci 1969;30(1):1–12.
[65] Borwankar R, Wasan D. The kinetics of adsorption of surface active agents at gas-liquid surfaces. Chem Eng Sci 1983;38(10):1637–49.
[66] Brosseau Q, Vrignon J, Baret J-C. Microfluidic dynamic interfacial tensiometry. Soft Matter 2014;10(17):3066–76.
[67] Rillaerts E, Joos P. Rate of demicellization from the dynamic surface tensions of micellar solutions. J Phys Chem 1982;86(17):3471–8.
[68] Danov K, Vlahovska P, Horozov T, Dushkin C, Kralchevsky P, Mehreteab A, et al. Adsorption from micellar surfactant solutions: nonlinear theory and experiment. J Colloid Interface Sci 1996;183(1):223–35.
[69] B. Noskov, "Kinetics of adsorption from micellar solutions," Adv Colloid Interface Sci, vol. 95, no. 2–3, pp. 237–293, 2002.
[70] Kresheck GC, Hamori E, Davenport G, Scheraga HA. Determination of the dissociation rate of dodecylpyridinium iodide micelles by a temperature-jump technique1a, b. J Am Chem Soc 1966;88(2):246–53.
[71] Nyrkova IA, Semenov AN. On the theory of micellization kinetics. Macromol Theor Simul 2005;14(9):569–85.
[72] Glawdel T, Ren CL. Droplet formation in microfluidic t-junction generators operating in the transitional regime. Iii. Dynamic surfactant effects. Physical Review E 2012;86(2):026308.
[73] Patist A, Kanicky JR, Shukla PK, Shah DO. Importance of micellar kinetics in relation to technological processes. J Colloid Interface Sci 2002;245(1):1–15.
[74] Fainerman V, Mys V, Makievski A, Petkov J, Miller R. Dynamic surface tension of micellar solutions in the millisecond and submillisecond time range. J Colloid Interface Sci 2006;302(1):40–6.
[75] Serrien G, Geeraerts G, Ghosh L, Joos P. Dynamic surface properties of adsorbed protein solutions: Bsa, casein and buttermilk. Colloids Surf 1992;68(4):219–33.
[76] Miller R, Fainerman V, Aksenenko E, Leser M, Michel M. Dynamic surface tension and adsorption kinetics of β-casein at the solution/air interface. Langmuir 2004;20(3):771–7.
[77] Fainerman V, Lucassen-Reynders E, Miller R. Description of the adsorption behaviour of proteins at water/fluid interfaces in the framework of a twodimensional solution model. Adv Colloid Interface Sci 2003;106(1–3):237–59.
[78] Ramírez P, Muñoz J, Fainerman V, Aksenenko E, Mucic N, Miller R. Dynamic interfacial tension of triblock copolymers solutions at the water–hexane interface. Colloids Surf A Physicochem Eng Asp 2011;391(1–3):119–24.
[79] Aidarova S, Sharipova A, Krägel J, Miller R. Polyelectrolyte/surfactant mixtures in the bulk and at water/oil interfaces. Adv Colloid Interface Sci 2014;205:87–93.
[80] Novikova AA, Vlasov PS, Lin S-Y, Sedláková Z, Noskov BA. Dynamic surface properties of poly (methylalkyldiallylammonium chloride) solutions. J Taiwan Inst Chem Eng 2017;80:122–7.
[81] Penfold J, Tucker I, Thomas R, Zhang J. Adsorption of polyelectrolyte/surfactant mixtures at the air-solution interface: poly (ethyleneimine)/sodium dodecyl sulfate. Langmuir 2005;21(22):10061–73.
[82] Mullins OC, Sabbah H, Eyssautier J, Pomerantz AE, Barré L, Andrews AB, et al. Advances in asphaltene science and the yen–Mullins model. Energy Fuel 2012;26(7):3986–4003.

[83] Langevin D, Argillier J-F. Interfacial behavior of asphaltenes. Adv Colloid Interface Sci 2016;233:83–93.
[84] Ferri JK, Stebe KJ. Which surfactants reduce surface tension faster? A scaling argument for diffusion-controlled adsorption. Adv Colloid Interface Sci 2000;85 (1):61–97.
[85] Pan R, Green J, Maldarelli C. Theory and experiment on the measurement of kinetic rate constants for surfactant exchange at an air/water interface. J Colloid Interface Sci 1998;205(2):213–30.
[86] Jin F, Balasubramaniam R, Stebe KJ. Surfactant adsorption to spherical particles: the intrinsic length scale governing the shift from diffusion to kinetic-controlled mass transfer. J Adhesion 2004;80(9):773–96.
[87] Alvarez NJ, Walker LM, Anna SL. A microtensiometer to probe the effect of radius of curvature on surfactant transport to a spherical interface. Langmuir ACS J Surf Colloids 2010;26(16):13310–9.
[88] Lin S-Y, Chang H-C, Chen E-M. The effect of bulk concentration on surfactant adsorption processes: the shift from diffusion-control to mixed kinetic-diffusion control with bulk concentration. J Chem Eng Japan 1996;29(4):634–41.
[89] Qazi MJ, Schlegel SJ, Backus EHG, Bonn M, Bonn D, Shahidzadeh N. Dynamic surface tension of surfactants in the presence of high salt concentrations. Langmuir ACS J Surf Colloids 2020;36(27):7956–64.
[90] Taylor CD, Valkovska DS, Bain CD. A simple and rapid method for the determination of the surface equations of state and adsorption isotherms for efficient surfactants. Phys Chem Chem Phys 2003;5(21):4885–91.
[91] Angarska J, Stubenrauch C, Manev E. Drainage of foam films stabilized with mixtures of non-ionic surfactants. Colloids Surf A Physicochem Eng Asp 2007;309 (1–3):189–97.
[92] He Y, Shang Y, Liu H, Langevin D, Salonen A. Surfactant adsorption onto interfaces: measuring the surface excess in time. Langmuir 2012;28(6):3146–51.
[93] Ybert C, Di Meglio J-M. Study of protein adsorption by dynamic surface tension measurements: diffusive regime. Langmuir 1998;14(2):471–5.
[94] Fainerman VB, Lylyk SV, Aksenenko EV, Liggieri L, Makievski AV, Petkov JT, et al. Adsorption layer characteristics of triton surfactants. Colloids Surf A Physicochem Eng Asp 2009;334(1–3):8–15.
[95] Fainerman V, Lylyk S, Aksenenko E, Makievski A, Petkov J, Yorke J, et al. Adsorption layer characteristics of triton surfactants: 1. Surface tension and adsorption isotherms. Colloids Surf A Physicochem Eng Asp 2009;334(1–3):1–7.
[96] Fainerman V, Lylyk S, Aksenenko E, Liggieri L, Makievski A, Petkov J, et al. Adsorption layer characteristics of triton surfactants: part 2. Dynamic surface tension and adsorption. Colloids Surf A Physicochem Eng Asp 2009;334(1–3): 8–15.
[97] Miller R, Aksenenko E, Fainerman V, Pison U. Kinetics of adsorption of globular proteins at liquid/fluid interfaces. Colloids Surf A Physicochem Eng Asp 2001; 183:381–90.
[98] Fainerman V, Miller R. 2. Thermodynamics of adsorption of surfactants at the fluid interfaces. In: Studies in interface science. vol. 13. Elsevier; 2001. p. 99–188.
[99] Fainerman V. Adsorption kinetics from concentrated micellar solutions of ionic surfactants at the water—air interface. Colloids Surf 1992;62(4):333–47.
[100] Fainerman V, Lucassen-Reynders E, Miller R. Adsorption of surfactants and proteins at fluid interfaces. Colloids Surf A Physicochem Eng Asp 1998;143(2–3): 141–65.
[101] Fainerman V, Zholob S, Lucassen-Reynders E, Miller R. Comparison of various models describing the adsorption of surfactant molecules capable of interfacial reorientation. J Colloid Interface Sci 2003;261(1):180–3.
[102] Lin S-Y, Tsay R-Y, Lin L-W, Chen S-I. Adsorption kinetics of c12e8 at the air-water interface: adsorption onto a clean interface. Langmuir 1996;12(26):6530–6.
[103] He Y, Yazhgur P, Salonen A, Langevin D. Adsorption–desorption kinetics of surfactants at liquid surfaces. Adv Colloid Interface Sci 2015;222:377–84.
[104] Zhmud BV, Tiberg F, Kizling J. Dynamic surface tension in concentrated solutions of c n e m surfactants: a comparison between the theory and experiment. Langmuir 2000;16(6):2557–65.
[105] Ferrari M, Liggieri L, Ravera F, Amodio C, Miller R. Adsorption kinetics of alkylphosphine oxides at water/hexane interface: 1. Pendant drop experiments. J Colloid Interface Sci 1997;186(1):40–5.
[106] Alvarez NJ, Vogus DR, Walker LM, Anna SL. Using bulk convection in a microtensiometer to approach kinetic-limited surfactant dynamics at fluid-fluid interfaces. J Colloid Interface Sci 2012;372(1):183–91.
[107] Thorsen T, Roberts RW, Arnold FH, Quake SR. Dynamic pattern formation in a vesicle-generating microfluidic device. Phys Rev Lett 2001;86(18):4163.
[108] Anna SL, Bontoux N, Stone HA. Formation of dispersions using "flow focusing" in microchannels. Appl Phys Lett 2003;82(3):364–6.
[109] Silverio V, Cardoso de Freitas S. Microfabrication techniques for microfluidic devices. Complex Fluid Flows Microfluidics 2018:25–51.
[110] Becker H, Gärtner C. Polymer microfabrication technologies for microfluidic systems. Anal Bioanal Chem 2008;390:89–111.
[111] Has C. Microfluidic approaches for measuring the interfacial tension in fluidfluid systems: a concise review. Int J Fluid Mech Res 2021;48(2):83–100.
[112] Kovalchuk NM, Simmons MJ. Review of the role of surfactant dynamics in drop microfluidics. Adv Colloid Interface Sci 2023;102844(312):6–13.
[113] Seemann R, Brinkmann M, Pfohl T, Herminghaus S. Droplet based microfluidics. Rep Prog Phys 2011;75(1):016601.
[114] Baret J-C. Surfactants in droplet-based microfluidics. Lab Chip 2012;12(3): 422–33.
[115] Anna SL. Droplets and bubbles in microfluidic devices. Annu Rev Fluid Mech 2016;48:285–309.
[116] Deng B, Schroën K, de Ruiter J. Dynamics of bubble formation in spontaneous microfluidic devices: controlling dynamic adsorption via liquid phase properties. J Colloid Interface Sci 2022;622:218–27.
[117] Guillot P, Colin A, Ajdari A. Stability of a jet in confined pressure-driven biphasic flows at low reynolds number in various geometries. In: Physical review. E, Statistical, Nonlinear, and Soft Matter Physics. vol. 78; 2008. p. 016307. no. 1 Pt 2.
[118] Moiré M, Peysson Y, Herzhaft B, Pannacci N, Gallaire F, Augello L, et al. Ultralow interfacial tension measurement through jetting/dripping transition. Langmuir 2017;33(10):2531–40.
[119] Liang X, Zhang J, Li M, Wang K, Luo G. Dynamic interfacial tension and adsorption kinetics of nonionic surfactants during microfluidic droplet formation process. Chem Eng J 2022;445:136658.
[120] van Dijke KC, Schroën K, van der Padt A, Boom R. Edge emulsification for food-grade dispersions. J Food Eng 2010;97(3):348–54.
[121] Sahin S, Bliznyuk O, Rovalino Cordova A, Schroën K. Microfluidic edge emulsification: the importance of interface interactions on droplet formation and pressure stability. Sci Rep 2016;6(1):26407.
[122] Muijlwijk K, Huang W, Vuist J-E, Berton-Carabin C, Schroën K. Convective mass transport dominates surfactant adsorption in a microfluidic y-junction. Soft Matter 2016;12(44):9025–9.
[123] Xu JH, Li S, Tan J, Luo G. Correlations of droplet formation in t-junction microfluidic devices: from squeezing to dripping. Microfluidics Nanofluidics 2008;5:711–7.
[124] T. Glawdel, C. Elbuken, and C. L. Ren, "Droplet formation in microfluidic t-junction generators operating in the transitional regime. i. experimental observations," *Physical Review E*, vol. 85, no. 1, p. 016322, 2012.
[125] T. Glawdel, C. Elbuken, and C. L. Ren, "Droplet formation in microfluidic t-junction generators operating in the transitional regime. ii. modeling," *Physical Review E*, vol. 85, no. 1, p. 016323, 2012.
[126] Wang K, Zhang L, Zhang W, Luo G. Mass-transfer-controlled dynamic interfacial tension in microfluidic emulsification processes. Langmuir ACS J Surf Colloids 2016;32(13):3174–85.
[127] Kalli M, Chagot L, Angeli P. Comparison of surfactant mass transfer with drop formation times from dynamic interfacial tension measurements in microchannels. J Colloid Interface Sci 2022;605:204–13.
[128] Van der Graaf S, Nisisako T, Schroën C, Van Der Sman R, Boom R. Lattice boltzmann simulations of droplet formation in a t-shaped microchannel. Langmuir 2006;22(9):4144–52.